Journal of the Mechanics and Physics of Solids 64 (2014) 61–82

Contents lists available at ScienceDirect

Journal of the Mechanics and Physics of Solids

journal homepage: www.elsevier.com/locate/jmps

Elastic dielectric composites: Theory and application to particle-filled ideal dielectrics

Oscar Lopez-Pamies*

Department of Civil and Environmental Engineering, University of Illinois, Urbana–Champaign, IL 61801, USA

ARTICLE INFO

Article history:
Received 7 May 2013
Received in revised form
29 September 2013
Accepted 30 October 2013
Available online 12 November 2013

Keywords:
Electroactive materials
Finite strain
Microstructures
Iterated homogenization

ABSTRACT

A microscopic field theory is developed with the aim of describing, explaining, and predicting the macroscopic response of elastic dielectric composites with two-phase particulate (periodic or random) microstructures under arbitrarily large deformations and electric fields. The central idea rests on the construction — via an iterated homogenization technique in finite electroelastostatics — of a specific but yet fairly general class of particulate microstructures which allow to compute exactly the homogenized response of the resulting composite materials. The theory is applicable to any choice of elastic dielectric behaviors (with possibly even or odd electroelastic coupling) for the underlying matrix and particles, and any choice of the one- and two-point correlation functions describing the microstructure. In spite of accounting for fine microscopic information, the required calculations amount to solving tractable first-order nonlinear (Hamilton-Jacobi-type) partial differential equations.

As a first application of the theory, explicit results are worked out for the basic case of ideal elastic dielectrics filled with initially spherical particles that are distributed either isotropically or in chain-like formations and that are ideal elastic dielectrics themselves. The effects that the permittivity, stiffness, volume fraction, and spatial distribution of the particles have on the overall electrostrictive deformation (induced by the application of a uniaxial electric field) of the composite are discussed in detail.

1. Introduction

Following their discovery in the 19th century (see, e.g., the historical review by Cady, 1946), deformable dielectrics have progressively enabled a wide variety of technologies. This has been particularly true for "hard" deformable dielectrics such as piezoelectrics (Uchino, 1997). Modern advances in organic materials have revealed that "soft" deformable dielectrics too hold tremendous potential to enable emerging technologies (Bar-Cohen, 2001; Carpi and Smela, 2009). At present, however, a major obstacle hindering the use of these soft active materials in actual devices is that they require — due to their inherent low permittivity — extremely high electric fields (>100 MV/m) to be actuated. Recent experiments have demonstrated that a promising solution to circumvent this limitation is to make composite materials, essentially by adding high-permittivity particles to the soft low-permittivity dielectrics (see, e.g., Zhang et al., 2002, 2007; Huang et al., 2005). Making composites out of hard deformable dielectrics has also proved increasingly beneficial for a broad range of applications (see, e.g., Akdogan et al., 2005). In this context, the objective of this work is to develop a microscopic field theory to describe, explain,

* Tel.: +1 217 244 1242.
E-mail address: pamies@illinois.edu

0022-5096/$ - see front matter © 2013 Elsevier Ltd. All rights reserved.
http://dx.doi.org/10.1016/j.jmps.2013.10.016

and predict the macroscopic behavior of deformable dielectric composites directly in terms of their microscopic behavior. Motivated by the above-referenced experimental observations, the focus shall be on *finite electroelastic deformations* of composites with *two-phase particulate microstructures*.

To put the problem at hand in perspective, we recall that a complete macroscopic or phenomenological theory describing the quasistatic electromechanical behavior of elastic dielectrics has been available since the foundational paper of Toupin (1956) in the 1950s. Motivated by the renewed interest in electroactive materials of the last 15 years, this theory has been reformulated and presented in a variety of more convenient forms by a number of researchers including Dorfmann and Ogden (2005), McMeeking and Landis (2005), Vu and Steinmann (2007), Fosdick and Tang (2007), Xiao and Bhattacharya (2008), Suo et al. (2008). By contrast, microscopic or homogenization theories — needed to deal with composite materials — have not been pursued to nearly the same extent. Among the few results available, there are the well-established *linear* results for piezoelectric composites (see, e.g., Milton, 2002 and references therein) and the *nonlinear* result for electrostrictive composites of Tian et al. (2012), both within the restricted context of *small deformations* and *small electric fields*. Within the general context of *finite deformations* and *finite electric fields*, the only explicit results available in the literature appear to be those of deBotton et al. (2007) for the overall electrostrictive response of two-phase laminates; see also the finite element results of Li and Landis (2012). There is also the more recent work of Ponte Castañeda and Siboni (2012) wherein a decoupling approximation is proposed to model a special class of elastic dielectrics filled with mechanically rigid particles.

We begin this work in Section 2 by formulating the electroelastostatics problem defining the macroscopic response of two-phase elastic dielectric particulate composites under arbitrarily large deformations and electric fields. By means of an iterated homogenization procedure, we construct in Section 3 a solution for this problem for a specific but yet fairly general class of two-phase particulate (periodic or random) microstructures. This solution — given implicitly by the first-order nonlinear partial differential equation (35)–(36) and described in detail in Section 3.3 — constitutes the main result of this paper. It is valid for any choice of elastic dielectric behaviors for the matrix and particles, and any choice of one- and two-point correlation functions describing the underlying microstructure. For demonstration purposes, we spell out in Section 4 its specialization to the case when the matrix material is an ideal elastic dielectric. This result is further specialized in Section 4.1 to the case when the particles are ideal elastic dielectrics themselves, initially spherical in shape and distributed either isotropically (Section 4.1.1) or in chain-like formations (Section 4.1.2). In Section 5, we present sample results for the overall electrostrictive deformation that these particle-filled ideal dielectrics undergo when they are exposed to a uniaxial electric field. The aim there is to shed light on how the presence of filler particles — in terms of their elastic dielectric properties, volume fraction, and spatial distribution — affect the electrostrictive performance of deformable dielectrics. Finally, we provide in A, B, and C further details regarding the microscopic field theory developed in Section 3, including how it can be utilized to extract information on local fields; knowledge of local fields is of the essence, for instance, to probe the onset of electromechanical instabilities such as cavitation and electric breakdown.

2. Problem formulation

Microscopic description of the material. Consider a heterogeneous material comprising a continuous matrix filled by a statistically uniform (i.e., translation invariant) distribution of firmly bonded particles that occupies a domain Ω_0, with boundary $\partial\Omega_0$, in its undeformed stress-free configuration. The matrix is labeled as phase $r=1$, while the particles are collectively labeled as phase $r=2$. The domains occupied by each individual phase are denoted by $\Omega_0^{(1)}$ and $\Omega_0^{(2)}$, so that $\Omega_0=\Omega_0^{(1)}\cup\Omega_0^{(2)}$ and their respective volume fractions are given by $c_0^{(1)}\doteq|\Omega_0^{(1)}|/|\Omega_0|$ and $c_0^{(2)}\doteq|\Omega_0^{(2)}|/|\Omega_0|$. We assume that the characteristic size of the particles is much smaller than the size of Ω_0 and, for convenience, choose units of length so that Ω_0 has unit volume.

Material points are identified by their initial position vector $\mathbf{X}$ in Ω_0 relative to some fixed point. Upon the application of mechanical and electrical stimuli, the position vector $\mathbf{X}$ of a material point moves to a new position specified by $\mathbf{x}=\chi(\mathbf{X})$, where χ is a one-to-one mapping from Ω_0 to the deformed configuration Ω. We assume that χ is twice continuously differentiable, except possibly on the particles/matrix boundaries. The associated deformation gradient is denoted by $\mathbf{F}=\mathrm{Grad}\,\chi$ and its determinant by $J=\det\mathbf{F}$.

Both the matrix ($r=1$) and the particles ($r=2$) are elastic dielectrics. We find it convenient to characterize their constitutive behaviors in a Lagrangian formulation by "total" free energies $W^{(r)}$ (suitably amended to include contributions from the Maxwell stress) per unit undeformed volume, as introduced by Dorfmann and Ogden (2005). In this work, such energy functions are assumed to be objective, differentiable, and, for definiteness, we shall use the deformation gradient $\mathbf{F}$ and Lagrangian electric field $\mathbf{E}$ as the independent variables[1]. It then follows that the first Piola–Kirchhoff stress tensor $\mathbf{S}$ and Lagrangian electric displacement $\mathbf{D}$ are given in terms of $\mathbf{F}$ and $\mathbf{E}$ simply by

$$\mathbf{S}=\frac{\partial W}{\partial\mathbf{F}}(\mathbf{X},\mathbf{F},\mathbf{E})\quad\text{and}\quad\mathbf{D}=-\frac{\partial W}{\partial\mathbf{E}}(\mathbf{X},\mathbf{F},\mathbf{E}),\tag{1}$$

[1] For our purposes here, it is equally convenient to use the Lagrangian electric displacement $\mathbf{D}$ as the electric independent variable instead of $\mathbf{E}$. For completeness, Appendix C includes a summary of results based on this alternative variable.

where

$$W(\mathbf{X},\mathbf{F},\mathbf{E}) = [1-\theta_0^{(2)}(\mathbf{X})]W^{(1)}(\mathbf{F},\mathbf{E}) + \theta_0^{(2)}(\mathbf{X})W^{(2)}(\mathbf{F},\mathbf{E}) \tag{2}$$

with $\theta_0^{(2)}(\mathbf{X})$ denoting the characteristic function of the regions occupied by the particles: $\theta_0^{(2)}(\mathbf{X}) = 1$ if $\mathbf{X} \in \Omega_0^{(2)}$ and zero otherwise. The total Cauchy stress $\mathbf{T}$, Eulerian electric displacement $\mathbf{D}$, and polarization $\mathbf{p}$ (per unit deformed volume) are in turn given by $\mathbf{T} = J^{-1}\mathbf{S}\mathbf{F}^T$, $\mathbf{d} = J^{-1}\mathbf{F}\mathbf{D}$, and $\mathbf{p} = \mathbf{d} - \varepsilon_0\mathbf{F}^{-T}\mathbf{E}$, where ε_0 stands for the permittivity of vacuum. We note that the objectivity of $W^{(r)}(\mathbf{Q}\mathbf{F},\mathbf{E}) = W^{(r)}(\mathbf{F},\mathbf{E})\ \forall \mathbf{Q} \in Orth^+$ ensures that $\mathbf{T}^T = \mathbf{T}$.

The characteristic function $\theta_0^{(2)}$ in (2) may be periodic or random. In the first case, its dependence on the position vector $\mathbf{X}$ is deterministically known once a unit cell and the lattice over which it is repeated are specified. In the second, the dependence of $\theta_0^{(2)}$ on $\mathbf{X}$ is only known in a probabilistic sense. In either case, at any rate, we shall ultimately require but partial knowledge of $\theta_0^{(2)}$ in terms of the one- and two-point correlation functions; see, e.g., Section II.A in Willis (1981), Chapter 15 in Milton (2002) for relevant discussions on correlation functions. In view of the assumed statistical uniformity of the microstructure, these functions are insensitive to translations and thus given by

$$p_0^{(2)} = \int_{\Omega_0} \theta_0^{(2)}(\mathbf{X})\,\mathrm{d}\mathbf{X} \quad \text{and} \quad p_0^{(22)}(\mathbf{Z}) = \int_{\Omega_0} \theta_0^{(2)}(\mathbf{Z}+\mathbf{X})\theta_0^{(2)}(\mathbf{X})\,\mathrm{d}\mathbf{X}. \tag{3}$$

Geometrically, the one-point correlation function $p_0^{(2)}$ represents the probability that a point lands in a particle when it is dropped randomly in Ω_0. In other words, $p_0^{(2)}$ is nothing more than the volume fraction of particles $c_0^{(2)}$ in the undeformed configuration. The two-point correlation function $p_0^{(22)}$ represents the probability that the ends of a rod of length and orientation described by the vector $\mathbf{Z}$ land within (the same or two different) particles when dropped randomly in Ω_0. Accordingly, $p_0^{(22)}$ contains finer information about the relative size, shape, and spatial distribution of the particles in the undeformed configuration.

The macroscopic response. In view of the separation of length scales and statistical uniformity of the microstructure, the above-defined elastic dielectric composite — though microscopically heterogeneous — is expected to behave macroscopically as a "homogenous" material. Following Hill (1972), its macroscopic or overall response is defined as the relation between the volume averages of the first Piola–Kirchhoff stress $\mathbf{S}$ and electric displacement $\mathbf{D}$ and the volume averages of the deformation gradient $\mathbf{F}$ and electric field $\mathbf{E}$ over the undeformed configuration Ω_0 when subjected to affine boundary conditions. Consistent with our choice of $\mathbf{F}$ and $\mathbf{E}$ as the independent variables, we consider the case of affine deformation and affine electric potential

$$\mathbf{x} = \overline{\mathbf{F}}\mathbf{X} \quad \text{and} \quad \varphi = -\overline{\mathbf{E}}\cdot\mathbf{X} \quad \text{on } \partial\Omega_0, \tag{4}$$

where the second-order tensor $\overline{\mathbf{F}}$ and vector $\overline{\mathbf{E}}$ stand for prescribed boundary data. In this case, it directly follows from the divergence theorem that $\int_{\Omega_0}\mathbf{F}(\mathbf{X})\,\mathrm{d}\mathbf{X} = \overline{\mathbf{F}}$ and $\int_{\Omega_0}\mathbf{E}(\mathbf{X})\,\mathrm{d}\mathbf{X} = \overline{\mathbf{E}}$, and hence the derivation of the macroscopic response reduces to finding the average stress $\overline{\mathbf{S}} \doteq \int_{\Omega_0}\mathbf{S}(\mathbf{X})\,\mathrm{d}\mathbf{X}$ and average electric displacement $\overline{\mathbf{D}} \doteq \int_{\Omega_0}\mathbf{D}(\mathbf{X})\,\mathrm{d}\mathbf{X}$. In direct analogy with the purely mechanical problem (Ogden, 1978), the result can be expediently written as

$$\overline{\mathbf{S}} = \frac{\partial \overline{W}}{\partial \overline{\mathbf{F}}}(\overline{\mathbf{F}},\overline{\mathbf{E}}) \quad \text{and} \quad \overline{\mathbf{D}} = -\frac{\partial \overline{W}}{\partial \overline{\mathbf{E}}}(\overline{\mathbf{F}},\overline{\mathbf{E}}), \tag{5}$$

where the scalar-valued function

$$\overline{W}(\overline{\mathbf{F}},\overline{\mathbf{E}}) = \min_{\mathbf{F}\in\mathcal{K}}\max_{\mathbf{E}\in\mathcal{E}} \int_{\Omega_0} W(\mathbf{X},\mathbf{F},\mathbf{E})\,\mathrm{d}\mathbf{X}, \tag{6}$$

henceforth referred to as the effective free energy function, corresponds physically to the total electroelastic free energy (per unit undeformed volume) of the composite. In this last expression, $\mathcal{K}$ and $\mathcal{E}$ denote sufficiently large sets of admissible deformation gradients and electric fields. Formally,

$$\mathcal{K} = \{\mathbf{F} :\ \exists\ \mathbf{x} = \boldsymbol{\chi}(\mathbf{X}) \text{ with } \mathbf{F} = \mathrm{Grad}\,\boldsymbol{\chi},\ J > 0 \text{ in } \Omega_0,\ \mathbf{x} = \overline{\mathbf{F}}\mathbf{X} \text{ on } \partial\Omega_0\} \tag{7}$$

and

$$\mathcal{E} = \{\mathbf{E} :\ \exists\ \varphi = \varphi(\mathbf{X}) \text{ with } \mathbf{E} = -\mathrm{Grad}\,\varphi \text{ in } \Omega_0,\ \varphi = -\overline{\mathbf{E}}\cdot\mathbf{X} \text{ on } \partial\Omega_0\}. \tag{8}$$

It is straightforward to show that the Euler–Lagrange equations associated with the variational problem (6) are nothing more than the equations of conservation of linear momentum and Gauss's law

$$\mathrm{Div}\,\mathbf{S} = \mathbf{0} \quad \text{and} \quad \mathrm{Div}\,\mathbf{D} = 0 \quad \text{in } \Omega_0. \tag{9}$$

The solution (assuming existence) of this coupled system of partial differential equations (pdes) is in general not unique. However, in the limit of small deformations and small electric fields, as $\overline{\mathbf{F}} \to \mathbf{I}$ and $\overline{\mathbf{E}} \to \mathbf{0}$, the solution is expected to be unique. As the applied deformation $\overline{\mathbf{F}}$ and/or electric field $\overline{\mathbf{E}}$ are increased beyond a small neighborhood of $\overline{\mathbf{F}} = \mathbf{I}$ and $\overline{\mathbf{E}} = \mathbf{0}$, such a unique solution may bifurcate into different energy solutions. This point corresponds to the onset of an instability. It is also worth remarking that the objectivity of the local energies $W^{(r)}$ directly implies that $\overline{W}$ is an objective function in the sense that $\overline{W}(\overline{\mathbf{Q}},\overline{\mathbf{F}},\overline{\mathbf{E}}) = \overline{W}(\overline{\mathbf{F}},\overline{\mathbf{E}})\ \forall \overline{\mathbf{Q}} \in Orth^+$. Moreover, in analogy with the local relations among Lagrangian and Eulerian

quantities, it follows that $\overline{\mathbf{T}}=\overline{J}^{-1}\overline{\mathbf{S}}\,\overline{\mathbf{F}}^{T}$, $\overline{\mathbf{d}}=\overline{J}^{-1}\overline{\mathbf{F}}\,\overline{\mathbf{D}}$, and $\overline{\mathbf{p}}=\overline{\mathbf{d}}-\varepsilon_0\overline{\mathbf{F}}^{-T}\overline{\mathbf{E}}$, where $\overline{\mathbf{T}}\doteq|\Omega|^{-1}\int_\Omega\mathbf{T}(\mathbf{x})\,d\mathbf{x}$, $\overline{\mathbf{d}}\doteq|\Omega|^{-1}\int_\Omega\mathbf{d}(\mathbf{x})\,d\mathbf{x}$, and $\overline{\mathbf{p}}\doteq|\Omega|^{-1}\int_\Omega\mathbf{p}(\mathbf{x})\,d\mathbf{x}$ are the volume averages of the total Cauchy stress $\mathbf{T}$, Eulerian electric displacement $\mathbf{d}$, and polarization $\mathbf{p}$ over the deformed configuration Ω, and where use has been made of the notation $\overline{J}=\det\overline{\mathbf{F}}$.

At this stage, it is important to emphasize that the computation of all bifurcated solutions of the Euler–Lagrange equations (9) — that is, all possible electromechanical instabilities — is in practice an impossibility, especially when the microstructure is random. Following common praxis in the purely mechanical context of finite elasticity, we circumvent this problem by adopting a semi-inverse approach in which the sets $\mathcal{K}$ and $\mathcal{E}$ of admissible deformation gradients and electric fields are restricted to include only certain subclasses of fields.[2] The idea is to exclude complicated bifurcated solutions associated with *local geometric* instabilities that might not have a significant effect on the macroscopic response of the composite; see Michel et al. (2010) for relevant work on local and global geometric instabilities. Formally, this amounts to considering an alternative definition of effective free energy function given by

$$\overline{W}^{\sharp}(\overline{\mathbf{F}},\overline{\mathbf{E}})=\min_{\mathbf{F}\in\mathcal{K}^{\sharp}}\max_{\mathbf{E}\in\mathcal{E}^{\sharp}}\int_{\Omega_0}W(\mathbf{X},\mathbf{F},\mathbf{E})\,d\mathbf{X},\tag{10}$$

where the minimization and maximization operations are now over suitably restricted sets $\mathcal{K}^{\sharp}$ and $\mathcal{E}^{\sharp}$ of deformation gradient tensors $\mathbf{F}$ and electric fields $\mathbf{E}$. The precise choice of restricted sets to be utilized in this work is described in the next section. From its definition, it is plain that $\overline{W}^{\sharp}=\overline{W}$ from the point $\overline{\mathbf{F}}=\mathbf{I}$, $\overline{\mathbf{E}}=\mathbf{0}$ all the way up to a first instability beyond which $\overline{W}^{\sharp}\neq\overline{W}$. For notational simplicity we will drop the use of the symbol $^{\sharp}$ in $\overline{W}$ henceforth, with the understanding that $\overline{W}$ will denote the electroelastic free energy defined in (10) unless otherwise stated.

3. An iterated homogenization theory

In order to generate solutions for (10), we pursue a "construction" strategy, one in which we devise a special but yet general family of characteristic functions $\theta_0^{(2)}$ that permit the exact computation of the resulting homogenization problem. Building on the techniques developed in Lopez-Pamies et al. (2011a) within the context of finite elasticity, the strategy comprises two main steps. The first step, described in Section 3.1, consists of an iterated dilute homogenization procedure (or differential scheme) in finite electroelastostatics. This procedure provides an implicit solution — in the form of a pde — for the effective free energy function of elastic dielectric composites with fairly general classes of microstructures in terms of an auxiliary dilute problem. The second step, described in Section 3.2, is concerned with the auxiliary dilute problem, which consists of the construction of a coated laminate of infinite rank whose matrix phase is present in dilute proportions in such a way that its effective free energy function can be determined exactly and explicitly up to a set of nonlinear algebraic equations. As laid out in Section 3.3, combining these two steps and specializing the result to the class of deformable dielectrics described in Section 2 leads to solutions for the effective free energy function $\overline{W}$, given directly in terms of $W^{(1)}$ and $W^{(2)}$, the one-point $p_0^{(2)}$ and two-point $p_0^{(22)}$ correlation functions of the (periodic or random) distribution of particles, and the applied loading conditions $\overline{\mathbf{F}}$ and $\overline{\mathbf{E}}$.

3.1. Iterated dilute homogenization in finite electroelastostatics

Iterated dilute homogenization methods are iterative techniques that employ results for the macroscopic properties of dilute composites in order to generate results for composites with finite volume fractions of constituents. The basic form of these techniques was introduced in the 1930s by Bruggeman (1935). Several decades later, Norris (1985) provided a more general formulation for material systems with more than two constituents and broader classes of microstructures, including granular microstructures; see also Avellaneda (1987) and Braides and Lukkassen (2000). To be useful, these techniques require knowledge of a dilute solution from which to start the iterative construction process. It is because of this requirement that most of the efforts reported to date have focused on the restricted context of linear problems where — as opposed to nonlinear problems — there is a wide variety of dilute solutions available. Nevertheless, the central idea of these techniques is geometrical in nature and can therefore be applied to any constitutively *coupled* and *nonlinear* problem of choice, provided, again, the availability of a relevant dilute solution. In the context of finite elasticity, Lopez-Pamies (2010) has recently put forward an iterated dilute homogenization formulation for the special case of two-phase composites. In this section, we extend this formulation to the coupled realm of finite electroelastostatics. For the sake of notational clarity, the derivation is presented for composites with three phases — from which the extension to an arbitrary number of phases becomes transparent — and then specialized to the case of two-phase particulate composites of interest here.

We begin by considering the domain Ω_0 to be initially occupied by a "backbone" material, which we label $r=0$ and take to be a homogeneous elastic dielectric characterized by a free energy function $W^{(0)}$ of arbitrary choice. We then embed a *dilute* (statistically uniform) distribution of materials $r=1$ and $r=2$, with infinitesimal volume fractions $v_1^{[1]}$ and $v_2^{[1]}$, in material 0 in such a way that the total volume of the system remains unaltered at $|\Omega_0|=1$. That is, we remove volumes $v_1^{[1]}$ and $v_2^{[1]}$ of material 0 and replace them with materials 1 and 2. Assuming a polynomial asymptotic behavior, the resulting

[2] Prominent examples include the subclasses of radially symmetric (see, e.g., Ball, 1982; Hashin, 1985) and piecewise constant (see, e.g., deBotton, 2005; Lopez-Pamies and Ponte Castañeda, 2009) fields.

composite material has an effective free energy function $\overline{W}^{[1]}$ of the form

$$\overline{W}^{[1]}(\overline{\mathbf{F}},\overline{\mathbf{E}}) = W^{(0)}(\overline{\mathbf{F}},\overline{\mathbf{E}}) + \mathcal{H}\{W^{(0)},W^{(1)},W^{(2)};\overline{\mathbf{F}},\overline{\mathbf{E}}\}v_1^{[1]} + \mathcal{G}\{W^{(0)},W^{(1)},W^{(2)};\overline{\mathbf{F}},\overline{\mathbf{E}}\}v_2^{[1]} \tag{11}$$

to order $O(1)$ in $v_1^{[1]}$ and $v_2^{[1]}$. Here, $\mathcal{H}$ and $\mathcal{G}$ are functionals with respect to their first three arguments, $W^{(0)}$, $W^{(1)}$ and $W^{(2)}$, and functions with respect to their last two arguments $\overline{\mathbf{F}}$ and $\overline{\mathbf{E}}$. The specific forms of $\mathcal{H}$ and $\mathcal{G}$ depend, of course, on the particular class of dilute distributions being considered.

Taking next the composite material with free energy function $\overline{W}^{[1]}$ — rather than $W^{(0)}$ — as the "backbone" material, we repeat exactly the same process of removal and replacing while keeping the volume fixed at $|\Omega_0| = 1$. This second iteration requires utilizing the same dilute distribution as in the first iteration, but with a larger length scale, since (11) is being employed as the free energy function of a "homogenous" elastic dielectric. Denoting by $v_1^{[2]}$ and $v_2^{[2]}$ the infinitesimal volume fractions of materials 1 and 2 embedded in this second step, the resulting composite material has now an effective free energy function that reads as

$$\overline{W}^{[2]}(\overline{\mathbf{F}},\overline{\mathbf{E}}) = \overline{W}^{[1]}(\overline{\mathbf{F}},\overline{\mathbf{E}}) + \mathcal{H}\{\overline{W}^{[1]},W^{(1)},W^{(2)};\overline{\mathbf{F}},\overline{\mathbf{E}}\}v_1^{[2]} + \mathcal{G}\{\overline{W}^{[1]},W^{(1)},W^{(2)};\overline{\mathbf{F}},\overline{\mathbf{E}}\}v_2^{[2]}. \tag{12}$$

We remark that the functionals $\mathcal{H}$ and $\mathcal{G}$ in (12) are the same as in (11) because we are considering *exactly the same*[3] dilute distributions. We further remark that the *total* volume fractions of materials 1 and 2 at this stage are given, respectively, by $\phi_1^{[2]} = v_1^{[2]} + \phi_1^{[1]}(1 - v_1^{[2]} - v_2^{[2]})$ and $\phi_2^{[2]} = v_2^{[2]} + \phi_2^{[1]}(1 - v_1^{[2]} - v_2^{[2]})$, where $\phi_1^{[1]} = v_1^{[1]}$ and $\phi_2^{[1]} = v_2^{[1]}$.

It is apparent now that repeating the same above process $n+1$ times, for arbitrarily large $n \in \mathbb{N}$, generates a composite material with effective free energy function

$$\overline{W}^{[n+1]}(\overline{\mathbf{F}},\overline{\mathbf{E}}) = \overline{W}^{[n]}(\overline{\mathbf{F}},\overline{\mathbf{E}}) + \mathcal{H}\{\overline{W}^{[n]},W^{(1)},W^{(2)};\overline{\mathbf{F}},\overline{\mathbf{E}}\}v_1^{[n+1]} + \mathcal{G}\{\overline{W}^{[n]},W^{(1)},W^{(2)};\overline{\mathbf{F}},\overline{\mathbf{E}}\}v_2^{[n+1]}, \tag{13}$$

which contains total volume fractions of materials 1 and 2 given by

$$\phi_1^{[n+1]} = v_1^{[n+1]} + \phi_1^{[n]}(1 - v_1^{[n+1]} - v_2^{[n+1]}), \quad \phi_2^{[n+1]} = v_2^{[n+1]} + \phi_2^{[n]}(1 - v_1^{[n+1]} - v_2^{[n+1]}). \tag{14}$$

Upon inverting equations (14) in favor of $v_1^{[n+1]}$ and $v_2^{[n+1]}$, relation (13) can be rewritten as the difference equation

$$\begin{aligned}\overline{W}^{[n+1]}(\overline{\mathbf{F}},\overline{\mathbf{E}}) - \overline{W}^{[n]}(\overline{\mathbf{F}},\overline{\mathbf{E}}) = {} & \frac{(1-\phi_2^{[n]})(\phi_1^{[n+1]} - \phi_1^{[n]}) + \phi_1^{[n]}(\phi_2^{[n+1]} - \phi_2^{[n]})}{1 - \phi_1^{[n]} - \phi_2^{[n]}} \mathcal{H}\{\overline{W}^{[n]},W^{(1)},W^{(2)};\overline{\mathbf{F}},\overline{\mathbf{E}}\} \\ & + \frac{(1-\phi_1^{[n]})(\phi_2^{[n+1]} - \phi_2^{[n]}) + \phi_2^{[n]}(\phi_1^{[n+1]} - \phi_1^{[n]})}{1 - \phi_1^{[n]} - \phi_2^{[n]}} \mathcal{G}\{\overline{W}^{[n]},W^{(1)},W^{(2)};\overline{\mathbf{F}},\overline{\mathbf{E}}\}.\end{aligned} \tag{15}$$

Taking now the limit of infinitely many iterations ($n \to \infty$) and parameterizing the construction process with a time-like variable $t \in [0,1]$, allows in turn to recast (15) as the pde

$$\begin{aligned}(1-\phi_1-\phi_2)\frac{\partial \overline{W}}{\partial t} = {} & \left[(1-\phi_2)\frac{\mathrm{d}\phi_1}{\mathrm{d}t} + \phi_1\frac{\mathrm{d}\phi_2}{\mathrm{d}t}\right]\mathcal{H}\{\overline{W},W^{(1)},W^{(2)};\overline{\mathbf{F}},\overline{\mathbf{E}}\} \\ & + \left[(1-\phi_1)\frac{\mathrm{d}\phi_2}{\mathrm{d}t} + \phi_2\frac{\mathrm{d}\phi_1}{\mathrm{d}t}\right]\mathcal{G}\{\overline{W},W^{(1)},W^{(2)};\overline{\mathbf{F}},\overline{\mathbf{E}}\}\end{aligned} \tag{16}$$

subject to the initial condition

$$\overline{W}(\overline{\mathbf{F}},\overline{\mathbf{E}},0) = W^{(0)}(\overline{\mathbf{F}},\overline{\mathbf{E}}), \tag{17}$$

for the effective free energy function, now written as $\overline{W} = \overline{W}(\overline{\mathbf{F}},\overline{\mathbf{E}},t)$. By construction, $\phi_1(t)$ and $\phi_2(t)$ in (16) are non-negative, non-decreasing, continuous functions such that $\phi_1(t)+\phi_2(t) \le 1$, $\phi_1(0) = \phi_2(0) = 0$, $\phi_1(1) = c_0^{(1)}$, and $\phi_2(1) = c_0^{(2)}$, but are arbitrary otherwise; here, it is recalled that $c_0^{(1)}$ and $c_0^{(2)}$ stand for the final volume fractions of materials 1 and 2 in the elastic dielectric composite. It is plain from (16) that the specific choice of functions $\phi_1(t)$ and $\phi_2(t)$ — and *not* just their final value $\phi_1(1) = c_0^{(1)}$ and $\phi_2(1) = c_0^{(2)}$ — dictates the construction path of the microstructure and thus greatly affects the form of the resulting effective free energy function $\overline{W}$.

The initial-value problem (16)–(17) provides an implicit framework for constructing solutions for the effective free energy function $\overline{W}$ of three-phase[4] elastic dielectric composites directly in terms of corresponding solutions — as characterized by the functionals $\mathcal{H}$ and $\mathcal{G}$ — when two constituents (here, $r=1$ and $r=2$) are present in dilute volume fractions. The framework is admittedly general in that it is applicable to any choice of free energy functions $W^{(0)}$, $W^{(1)}$, $W^{(2)}$ and broad classes of microstructures, including granular and particulate microstructures. To be useful, however, the framework (16)–(17) requires knowledge of the functionals $\mathcal{H}$ and $\mathcal{G}$ describing the dilute electroelastic response of the microstructures of interest, which is in general a notable challenge.

Specialization to two-phase particulate microstructures. The focus of this paper is on elastic dielectric composites with two-phase particulate microstructures, where, again, material $r=1$ plays the role of the matrix while material $r=2$ plays the role of the particles. In this regard, for reasons that will become apparent further below, we shall select the "backbone"

[3] More elaborate construction processes can be easily devised, but such a degree of generality is unnecessary here.
[4] The generalization to any number of phases follows from a trivial extension of steps (11)–(15).

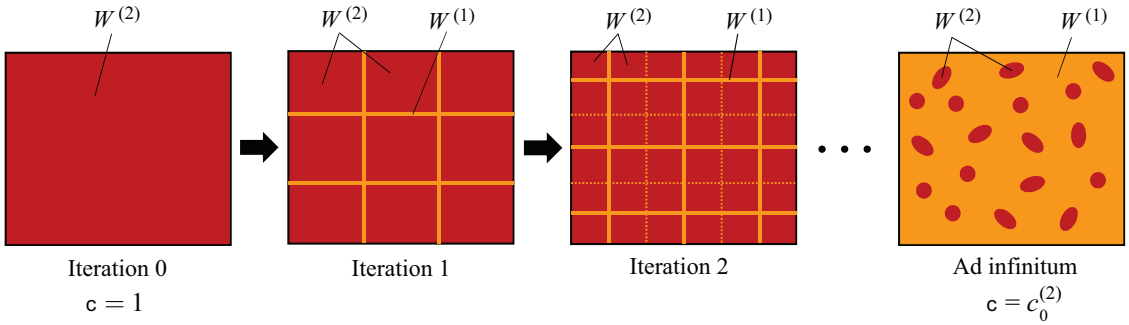

Fig. 1. Schematic of the iterative construction process of a two-phase particulate microstructure where matrix material, with free energy $W^{(1)}$, is continuously added at each step of the process in such a way that the total volume fraction of particles, with free energy $W^{(2)}$, reduces from its initial value of $c=1$ to the desired final value of $c=c_0^{(2)}$.

material in the above-developed framework to be identical to that of the particles, so that $W^{(0)}=W^{(2)}$. And consider construction paths characterized by the functions $\phi_2(t)=0$ and $\phi_1(t)=c_0^{(1)}t \doteq 1-c$, where $c\in[c_0^{(2)},1]$ is a concentration-like variable preferred here over t as the parameterizing variable. That is, we start out with an elastic dielectric particulate composite whose matrix is present in dilute volume fraction and then continuously add matrix material at each step of the construction process in such a way that the total volume fraction of particles reduces from its initial value of $c=1$ to the desired final value of $c=c_0^{(2)}$; Fig. 1 illustrates schematically this process. With a slight abuse of notation, the formulation (16)–(17) reduces in this case to the initial-value problem

$$c\frac{\partial \overline{W}}{\partial c}+\mathcal{H}\{W^{(1)},\overline{W};\overline{\mathbf{F}},\overline{\mathbf{E}}\}=0 \quad \text{with } \overline{W}(\overline{\mathbf{F}},\overline{\mathbf{E}},1)=W^{(2)}(\overline{\mathbf{F}},\overline{\mathbf{E}}), \tag{18}$$

for the effective free energy function $\overline{W}=\overline{W}(\overline{\mathbf{F}},\overline{\mathbf{E}},c_0^{(2)})$, where we emphasize that the integration of the pde $(18)_1$ must be carried out from $c=1$ to the final value of volume fraction of particles $c=c_0^{(2)}$ of interest.

3.2. The auxiliary dilute problem: coated laminates with dilute volume fraction of matrix

Having established the generic result (18), our next objective is to devise a specific form for the functional $\mathcal{H}$. To this end, we make use of the coated or sequential laminates originally introduced by Francfort and Murat (1986), following the lead of Tartar (1985), in linear elasticity. Remarkably, this class of microstructures permits the construction of two-phase particulate laminates of *infinite rank* whose effective — possibly coupled and nonlinear — properties can be determined *exactly* and *explicitly* (up to a set of algebraic equations) in the limit when the *matrix phase* is present in dilute volume fractions.[5] This powerful attribute was originally recognized by Idiart (2008), following seminal work of deBotton (2005), in the context of small-strain nonlinear elasticity. In this section, we work out the extension of these results to the coupled realm of finite electroelastostatics.

The starting point is to consider the homogenization problem (10) of a two-phase rank-1 laminate, made up of alternating layers of elastic dielectric materials $r=1$ and $r=2$ with volume fractions $(1-f^{[1]})$ and $f^{[1]}$, respectively, and with lamination direction given by the vector $\boldsymbol{\xi}^{[1]}$, of unit length but arbitrary otherwise. Fig. 2(a) provides an schematic of such a laminate and of its defining quantities. Throughout this subsection, volume fractions and lamination directions refer to the undeformed configuration Ω_0, and a superscript[6] $[i]$ is used to mark quantities associated with a laminate of rank i. Because of the one-dimensionality of the heterogeneity in the direction $\boldsymbol{\xi}^{[1]}$ — similar to the classical linear context (see, e.g., Chapter 9 in Milton, 2002) — the relevant Euler–Lagrange equations (9) admit *piecewise constant solutions* of the form

$$\mathbf{F}(\mathbf{X})=\begin{cases}\mathbf{F}^{(1)}=\overline{\mathbf{F}}+f^{[1]}\,\boldsymbol{\alpha}^{[1]}\otimes\boldsymbol{\xi}^{[1]} & \text{if } \mathbf{X}\in\Omega_0^{(1)}\\ \mathbf{F}^{(2)}=\overline{\mathbf{F}}-(1-f^{[1]})\boldsymbol{\alpha}^{[1]}\otimes\boldsymbol{\xi}^{[1]} & \text{if } \mathbf{X}\in\Omega_0^{(2)}\end{cases}, \tag{19}$$

and

$$\mathbf{E}(\mathbf{X})=\begin{cases}\mathbf{E}^{(1)}=\overline{\mathbf{E}}+f^{[1]}\beta^{[1]}\boldsymbol{\xi}^{[1]} & \text{if } \mathbf{X}\in\Omega_0^{(1)}\\ \mathbf{E}^{(2)}=\overline{\mathbf{E}}-(1-f^{[1]})\beta^{[1]}\boldsymbol{\xi}^{[1]} & \text{if } \mathbf{X}\in\Omega_0^{(2)}\end{cases} \tag{20}$$

[5] The more intuitive dilute limit of particles does *not* permit for such an analytically explicit treatment, as the limit of infinite rank remains elusive in that case.

[6] The use of similar notation to that of Section 3.1 should not lead to confusion.

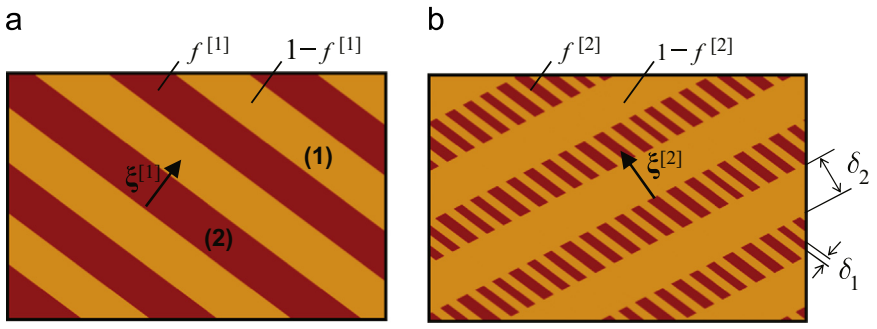

Fig. 2. (a) Illustration of a two-phase rank-1 laminate with volume fractions $(1-f^{[1]})$ and $f^{[1]}$ of materials $r=1$ and $r=2$, respectively, and lamination direction $\boldsymbol{\xi}^{[1]}$. (b) A coated rank-2 laminate wherein the underlying rank-1 laminate is much smaller in length scale: $\delta_2 \gg \delta_1$.

for some arbitrary vector $\boldsymbol{\alpha}^{[1]}$ and scalar $\beta^{[1]}$. Upon choosing the sets $\mathcal{K}^{\sharp}$ and $\mathcal{E}^{\sharp}$ in (10) to include solely piecewise constant deformation gradients and electric fields, the effective free energy function of the rank-1 laminate specializes then to

$$\overline{W}^{[1]}(\overline{\mathbf{F}},\overline{\mathbf{E}}) = \min_{\boldsymbol{\alpha}^{[1]}} \max_{\beta^{[1]}} \{(1-f^{[1]})W^{(1)}(\mathbf{F}^{(1)},\mathbf{E}^{(1)}) + f^{[1]}\, W^{(2)}(\mathbf{F}^{(2)},\mathbf{E}^{(2)})\}. \tag{21}$$

The minimization condition with respect to $\boldsymbol{\alpha}^{[1]}$ implies mechanical equilibrium whereas the maximization with respect to $\beta^{[1]}$ implies Gauss's law across material interfaces. Namely, they imply the jump conditions $[\partial W^{(1)}(\mathbf{F}^{(1)},\mathbf{E}^{(1)})/\partial \mathbf{F}]\boldsymbol{\xi}^{[1]} = [\partial W^{(2)}(\mathbf{F}^{(2)},\mathbf{E}^{(2)})/\partial \mathbf{F}]\boldsymbol{\xi}^{[1]}$ and $[\partial W^{(1)}(\mathbf{F}^{(1)},\mathbf{E}^{(1)})/\partial \mathbf{E}]\cdot\boldsymbol{\xi}^{[1]} = [\partial W^{(2)}(\mathbf{F}^{(2)},\mathbf{E}^{(2)})/\partial \mathbf{E}]\cdot\boldsymbol{\xi}^{[1]}$.

Next, we consider a rank-2 laminate made up by layering material 1 with the above rank-1 laminate along lamination direction $\boldsymbol{\xi}^{[2]}$. As shown schematically in Fig. 2(b), this choice of construction process leads to a two-phase particulate microstructure, one where material 1 plays the role of the matrix (i.e., continuous) phase and material 2 plays the role of the particle (i.e., discontinuous) phase. We take the length scale of the lower-rank laminate to be much smaller than the length scale of the higher-rank laminate — depicted as $\delta_1 \ll \delta_2$ in Fig. 2(b) — so that in the rank-2 laminate, the rank-1 laminate can be regarded as a "homogeneous" elastic dielectric. Granted this separation-of-length-scales hypothesis and restricting attention again to piecewise constant deformation gradients and electric fields, the effective free energy function $\overline{W}^{[2]}$ of the rank-2 laminate is given by an expression analogous to (21), with $W^{(2)}$ replaced by $\overline{W}^{[1]}$. More specifically, denoting by $(1-f^{[2]})$ and $f^{[2]}$ the volume fractions of material 1 and rank-1 laminate, the effective free energy function of the resulting rank-2 laminate is given by

$$\begin{aligned}\overline{W}^{[2]}(\overline{\mathbf{F}},\overline{\mathbf{E}}) = \min_{\boldsymbol{\alpha}^{[2]}} \max_{\beta^{[2]}} \Big\{ & (1-f^{[2]})W^{(1)}(\overline{\mathbf{F}} + f^{[2]}\boldsymbol{\alpha}^{[2]} \otimes \boldsymbol{\xi}^{[2]}, \overline{\mathbf{E}} + f^{[2]}\beta^{[2]}\boldsymbol{\xi}^{[2]}) \\ & + f^{[2]}\overline{W}^{[1]}(\overline{\mathbf{F}} - (1-f^{[2]})\boldsymbol{\alpha}^{[2]} \otimes \boldsymbol{\xi}^{[2]}, \overline{\mathbf{E}} - (1-f^{[2]})\beta^{[2]}\boldsymbol{\xi}^{[2]}) \Big\}.\end{aligned} \tag{22}$$

The *total* volume fraction of material 2 in this rank-2 laminate is given by $c_0^{(2)} = f^{[1]}f^{[2]}$ and that of material 1 by $c_0^{(1)} = 1-c_0^{(2)} = 1-f^{[1]}f^{[2]}$.

Repeating the same above process an arbitrary number of times $m \in \mathbb{N}$ — always laminating material 1 with the preceding rank-i laminate in proportions $(1-f^{[i]})$ and $f^{[i]}$, respectively, along a lamination direction $\boldsymbol{\xi}^{[i]}$ — generates a rank-m laminate whose effective free energy function $\overline{W}^{[m]}$ can be deduced from recurrent use of the basic formula (21) with (19)–(20) for rank-1 laminates. After some algebraic manipulations, the result reads as

$$\overline{W}^{[m]}(\overline{\mathbf{F}},\overline{\mathbf{E}}) = \min_{\substack{\boldsymbol{\alpha}^{[i]} \\ i=1,\dots,m}} \max_{\substack{\beta^{[i]} \\ i=1,\dots,m}} \left\{ \left(\prod_{i=1}^{m} f^{[i]} \right) W^{(2)}\left(\overline{\mathbf{F}}^{(2)}, \overline{\mathbf{E}}^{(2)}\right) + \sum_{i=1}^{m} \frac{1-f^{[i]}}{f^{[i]}} \left(\prod_{j=i}^{m} f^{[j]} \right) W^{(1)}\left(\mathbf{F}^{[i]}, \mathbf{E}^{[i]}\right) \right\}, \tag{23}$$

where the deformation gradient tensors $\mathbf{F}^{[i]}$ and $\overline{\mathbf{F}}^{(2)}$ are given by

$$\mathbf{F}^{[i]} = \overline{\mathbf{F}} + \boldsymbol{\alpha}^{[i]} \otimes \boldsymbol{\xi}^{[i]} - \sum_{j=i}^{m} (1-f^{[j]})\boldsymbol{\alpha}^{[j]} \otimes \boldsymbol{\xi}^{[j]}, \quad i = 1,\dots,m, \tag{24}$$

$$\overline{\mathbf{F}}^{(2)} = \overline{\mathbf{F}} - \sum_{j=1}^{m} (1-f^{[j]})\boldsymbol{\alpha}^{[j]} \otimes \boldsymbol{\xi}^{[j]}, \tag{25}$$

and the electric field vectors $\mathbf{E}^{[i]}$ and $\overline{\mathbf{E}}^{(2)}$ by

$$\mathbf{E}^{[i]} = \overline{\mathbf{E}} + \beta^{[i]}\boldsymbol{\xi}^{[i]} - \sum_{j=i}^{m} (1-f^{[j]})\beta^{[j]}\boldsymbol{\xi}^{[j]}, \quad i = 1,\dots,m, \tag{26}$$

$$\overline{\mathbf{E}}^{(2)} = \overline{\mathbf{E}} - \sum_{j=1}^{m} (1-f^{[j]})\beta^{[j]}\boldsymbol{\xi}^{[j]}. \tag{27}$$

The total volume fraction of material 2 (i.e., the particles) in this rank-m laminate is given by $c_0^{(2)} = \prod_{i=1}^{m} f^{[i]}$ and that of material 1 (i.e., the matrix) by $c_0^{(1)} = 1 - c_0^{(2)} = 1 - \prod_{i=1}^{m} f^{[i]}$. And, again, each iteration step in the above construction process makes use of sets of kinematically and electrically admissible fields, $\mathcal{K}^\sharp$ and $\mathcal{E}^\sharp$, that include only piecewise constant deformation gradients and electric fields.

The final step in this part of the derivation is to take the limit of dilute volume fraction of matrix material $c_0^{(1)} \to 0$ in the result (23). To this end, following deBotton (2005) and Idiart (2008), it proves helpful to introduce the parametrization

$$f^{[i]} = 1 - \nu^{[i]} c_0^{(1)} \quad \text{with } \nu^{[i]} \geq 0, \quad \sum_{i=1}^{m} \nu^{[i]} = 1. \tag{28}$$

Substituting expression (28) in (23) and taking the limit as $c_0^{(1)} \to 0$ leads to

$$\begin{aligned}\overline{W}^{[m]}(\overline{\mathbf{F}},\overline{\mathbf{E}}) = W^{(2)}(\overline{\mathbf{F}},\overline{\mathbf{E}}) - \Bigg\{ W^{(2)}(\overline{\mathbf{F}},\overline{\mathbf{E}}) + \max_{\substack{\boldsymbol{\alpha}^{[i]} \\ i=1,\ldots,m}} \min_{\substack{\beta^{[i]} \\ i=1,\ldots,m}} \Bigg\{ \sum_{i=1}^{m} \Bigg[\boldsymbol{\alpha}^{[i]} \cdot \frac{\partial W^{(2)}}{\partial \overline{\mathbf{F}}}(\overline{\mathbf{F}},\overline{\mathbf{E}})\boldsymbol{\xi}^{[i]} \\ + \beta^{[i]} \frac{\partial W^{(2)}}{\partial \overline{\mathbf{E}}}(\overline{\mathbf{F}},\overline{\mathbf{E}}) \cdot \boldsymbol{\xi}^{[i]} - W^{(1)}\left(\overline{\mathbf{F}} + \boldsymbol{\alpha}^{[i]} \otimes \boldsymbol{\xi}^{[i]}, \overline{\mathbf{E}} + \beta^{[i]}\boldsymbol{\xi}^{[i]}\right) \Bigg] \nu^{[i]} \Bigg\} \Bigg\} c_0^{(1)} + O\left((c_0^{(1)})^2\right),\end{aligned} \tag{29}$$

where we have assumed that the asymptotic behaviors of the maximizing vectors $\boldsymbol{\alpha}^{[i]}$ and minimizing scalars $\beta^{[i]}$ have a regular polynomial form with leading term of order[7] $O((c_0^{(1)})^0)$. Introducing further the generalized function

$$\nu(\boldsymbol{\xi}) = \sum_{i=1}^{m} \nu^{[i]}\, \delta(\boldsymbol{\xi} - \boldsymbol{\xi}^{[i]}) \tag{30}$$

with $\delta(\boldsymbol{\xi})$ denoting the Dirac delta function, allows to rewrite the result (29) more compactly as

$$\begin{aligned}\overline{W}(\overline{\mathbf{F}},\overline{\mathbf{E}}) = W^{(2)}(\overline{\mathbf{F}},\overline{\mathbf{E}}) - \Bigg\{ W^{(2)}(\overline{\mathbf{F}},\overline{\mathbf{E}}) + \int_{|\boldsymbol{\xi}|=1} \max_{\boldsymbol{\alpha}} \min_{\beta} \Bigg[\boldsymbol{\alpha} \cdot \frac{\partial W^{(2)}}{\partial \mathbf{F}}(\overline{\mathbf{F}},\overline{\mathbf{E}})\boldsymbol{\xi} + \beta \frac{\partial W^{(2)}}{\partial \mathbf{E}}(\overline{\mathbf{F}},\overline{\mathbf{E}}) \cdot \boldsymbol{\xi} \\ - W^{(1)}(\overline{\mathbf{F}} + \boldsymbol{\alpha} \otimes \boldsymbol{\xi}, \overline{\mathbf{E}} + \beta\boldsymbol{\xi}) \Bigg] \nu(\boldsymbol{\xi})\, \mathrm{d}\boldsymbol{\xi} \Bigg\} c_0^{(1)} + O((c_0^{(1)})^2),\end{aligned} \tag{31}$$

where the superscript $[m]$ has been dropped for notational simplicity. As it stands, expression (31) is valid for laminates of *finite* as well as *infinite* rank: in the second case, $\nu(\boldsymbol{\xi})$ is a continuous function of $\boldsymbol{\xi}$. The fact that the result (31) is valid for infinite-rank laminates is of chief importance as it allows to consider — contrary to finite-rank laminates — general classes of microstructures, including the practical cases of isotropic, transversely isotropic, and orthotropic microstructures.

From the constraint $(28)_3$, it follows that the function $\nu(\boldsymbol{\xi})$ integrates to unity, $\int_{|\boldsymbol{\xi}|=1} \nu(\boldsymbol{\xi})\, \mathrm{d}\boldsymbol{\xi} = 1$, and so the integral in (31) corresponds to nothing more than to a weighted orientational average. To ease notation, we introduce

$$\langle\, \cdot\, \rangle \doteq \int_{|\boldsymbol{\xi}|=1} (\cdot)\nu(\boldsymbol{\xi})\, \mathrm{d}\boldsymbol{\xi}. \tag{32}$$

The result (31) can thus be finally written, to order $O(c_0^{(1)})$, as

$$\overline{W}(\overline{\mathbf{F}},\overline{\mathbf{E}}) = W^{(2)}(\overline{\mathbf{F}},\overline{\mathbf{E}}) + \mathcal{H}\{W^{(1)}, W^{(2)}; \overline{\mathbf{F}},\overline{\mathbf{E}}\} c_0^{(1)} \tag{33}$$

with

$$\mathcal{H}\{W^{(1)}, W^{(2)}; \overline{\mathbf{F}},\overline{\mathbf{E}}\} = -W^{(2)}(\overline{\mathbf{F}},\overline{\mathbf{E}}) - \left\langle \max_{\boldsymbol{\alpha}} \min_{\beta} \left[\boldsymbol{\alpha} \cdot \frac{\partial W^{(2)}}{\partial \mathbf{F}}(\overline{\mathbf{F}},\overline{\mathbf{E}})\boldsymbol{\xi} + \beta \frac{\partial W^{(2)}}{\partial \mathbf{E}}(\overline{\mathbf{F}},\overline{\mathbf{E}}) \cdot \boldsymbol{\xi} - W^{(1)}(\overline{\mathbf{F}} + \boldsymbol{\alpha} \otimes \boldsymbol{\xi}, \overline{\mathbf{E}} + \beta\boldsymbol{\xi}) \right] \right\rangle. \tag{34}$$

Expression (33) with (34) constitutes an asymptotically exact result for the effective free energy function of a two-phase elastic dielectric composite with particulate microstructure where the matrix material $r=1$ is present in dilute volume fraction. The specifics of the microstructure enter the result through the volume fraction of particles $c_0^{(2)} = 1 - c_0^{(1)}$ and the function $\nu(\boldsymbol{\xi})$. The geometrical meaning of the latter is detailed in the sequel.

3.3. The effective free energy function $\overline{W}$

We are now in a position to generate solutions for the effective free energy function (10) of two-phase elastic dielectric composites with fairly general classes of (periodic and random) particulate microstructures. Indeed, direct use of the functional (34) in the iterative framework (18) leads to a solution for $\overline{W} = \overline{W}(\overline{\mathbf{F}},\overline{\mathbf{E}},c_0^{(2)})$ given implicitly by the first-order

[7] This is indeed the case for most free energies $W^{(1)}$ and $W^{(2)}$ of practical interest.

nonlinear pde

$$c\frac{\partial \overline{W}}{\partial c}-\overline{W}-\left\langle \max_{\boldsymbol{\alpha}}\min_{\beta}\left[\boldsymbol{\alpha}\cdot\frac{\partial \overline{W}}{\partial \overline{\mathbf{F}}}\,\boldsymbol{\xi}+\beta\frac{\partial \overline{W}}{\partial \overline{\mathbf{E}}}\cdot\boldsymbol{\xi}-W^{(1)}(\overline{\mathbf{F}}+\boldsymbol{\alpha}\otimes\boldsymbol{\xi},\overline{\mathbf{E}}+\beta\boldsymbol{\xi})\right]\right\rangle=0 \tag{35}$$

subject to the initial condition

$$\overline{W}(\overline{\mathbf{F}},\overline{\mathbf{E}},1)=W^{(2)}(\overline{\mathbf{F}},\overline{\mathbf{E}}), \tag{36}$$

where, again, the triangular brackets denote the orientational average (32) and the integration of the pde (35) is to be carried out from $c=1$ to the desired final value of volume fraction of particles $c=c_0^{(2)}$. The result (35)–(36) depends on the microstructure through $c_0^{(2)}$ and $\nu(\boldsymbol{\xi})$. While the volume fraction $c_0^{(2)}$ can be identified identically with the one-point correlation function $(3)_1$, the function $\nu(\boldsymbol{\xi})$ can be shown to be directly related to the two-point correlation function $(3)_2$. To see this connection, following common practice (Brown, 1955; Chapter 15 in Milton, 2002), it suffices to consider the limit of weak inhomogeneity in (35)–(36). The details are presented in Appendix A, but the results can be simply summarized as follows:

- *Periodic microstructures*. For the case of periodic distributions of particles, denoting by Q_0 and

$$\mathcal{R}=\{\mathbf{Y}:\mathbf{Y}=n_1\mathbf{A}_1+n_2\mathbf{A}_2+n_3\mathbf{A}_3,\ n_i\in\mathbb{Z}\} \tag{37}$$

the repeating unit cell and associated lattice chosen to describe the microstructure, the function $\nu(\boldsymbol{\xi})$ takes the form

$$\nu(\boldsymbol{\xi})=\sum_{\mathbf{k}\in\mathcal{R}^*-\{\mathbf{0}\}}\frac{\widehat{p}_0^{(22)}(\mathbf{k})}{c_0^{(1)}c_0^{(2)}}\,\delta\left(\boldsymbol{\xi}-\frac{\mathbf{k}}{|\mathbf{k}|}\right)\quad\text{with }\widehat{p}_0^{(22)}(\mathbf{k})=\frac{1}{|Q_0|}\int_{Q_0}p_0^{(22)}(\mathbf{X})e^{-i\mathbf{X}\cdot\mathbf{k}}\,d\mathbf{X}, \tag{38}$$

where $\mathcal{R}^*$ stands for the reciprocal lattice in Fourier space

$$\mathcal{R}^*=\{\mathbf{k}:\mathbf{k}=n_1\mathbf{B}_1+n_2\mathbf{B}_2+n_3\mathbf{B}_3,\quad n_i\in\mathbb{Z}\} \tag{39}$$

with

$$\mathbf{B}_1=2\pi\frac{\mathbf{A}_2\wedge\mathbf{A}_3}{\mathbf{A}_1\cdot(\mathbf{A}_2\wedge\mathbf{A}_3)},\quad \mathbf{B}_2=2\pi\frac{\mathbf{A}_3\wedge\mathbf{A}_1}{\mathbf{A}_1\cdot(\mathbf{A}_2\wedge\mathbf{A}_3)},\quad \mathbf{B}_3=2\pi\frac{\mathbf{A}_1\wedge\mathbf{A}_2}{\mathbf{A}_1\cdot(\mathbf{A}_2\wedge\mathbf{A}_3)}. \tag{40}$$

Direct use of relation (38) allows to rewrite the pde (35) more explicitly as

$$c\frac{\partial \overline{W}}{\partial c}-\overline{W}-\sum_{\substack{\mathbf{k}\in\mathcal{R}^*-\{\mathbf{0}\}\\ \boldsymbol{\xi}=\mathbf{k}/|\mathbf{k}|}}\left\{\max_{\boldsymbol{\alpha}}\min_{\beta}\left[\boldsymbol{\alpha}\cdot\frac{\partial \overline{W}}{\partial \overline{\mathbf{F}}}\boldsymbol{\xi}+\beta\frac{\partial \overline{W}}{\partial \overline{\mathbf{E}}}\cdot\boldsymbol{\xi}-W^{(1)}(\overline{\mathbf{F}}+\boldsymbol{\alpha}\otimes\boldsymbol{\xi},\overline{\mathbf{E}}+\beta\boldsymbol{\xi})\right]\frac{|\widehat{\theta}_0^{(2)}(\mathbf{k})|^2}{c_0^{(1)}c_0^{(2)}}\right\}=0, \tag{41}$$

where we have utilized the fact that $\widehat{p}_0^{(22)}(\mathbf{k})=|\widehat{\theta}_0^{(2)}(\mathbf{k})|^2$ with $\widehat{\theta}_0^{(2)}(\mathbf{k})=|Q_0|^{-1}\int_{Q_0}\theta_0^{(2)}(\mathbf{X})e^{-i\mathbf{k}\cdot\mathbf{X}}\,d\mathbf{X}$ denoting the Fourier transform of the characteristic function $\theta_0^{(2)}$.
- *Random microstructures*. For the case of random distributions of particles, the function $\nu(\boldsymbol{\xi})$ takes the form

$$\nu(\boldsymbol{\xi})=-\frac{1}{8\pi^2}\int_{\Omega_0}h(\mathbf{X})\delta''(\boldsymbol{\xi}\cdot\mathbf{X})\,d\mathbf{X}\quad\text{with }h(\mathbf{X})=\frac{p_0^{(22)}(\mathbf{X})-(c_0^{(2)})^2}{c_0^{(1)}c_0^{(2)}}, \tag{42}$$

where h is the so-called scaled autocovariance and δ'' denotes the second derivative of the Dirac delta function with respect to its scalar argument $\boldsymbol{\xi}\cdot\mathbf{X}$.
Direct use of relation (42) allows to rewrite the pde (35) more explicitly as

$$c\frac{\partial \overline{W}}{\partial c}-\overline{W}+\frac{1}{8\pi^2}\int_{|\boldsymbol{\xi}|=1}\int_{\Omega_0}\max_{\boldsymbol{\alpha}}\min_{\beta}\left[\boldsymbol{\alpha}\cdot\frac{\partial \overline{W}}{\partial \overline{\mathbf{F}}}\,\boldsymbol{\xi}+\beta\frac{\partial \overline{W}}{\partial \overline{\mathbf{E}}}\cdot\boldsymbol{\xi}\quad -W^{(1)}(\overline{\mathbf{F}}+\boldsymbol{\alpha}\otimes\boldsymbol{\xi},\overline{\mathbf{E}}+\beta\boldsymbol{\xi})\right]h(\mathbf{X})\delta''(\boldsymbol{\xi}\cdot\mathbf{X})\,d\mathbf{X}\,d\boldsymbol{\xi}=0. \tag{43}$$

The following comments are in order:

(i) *Electroelastic behavior of the matrix and particles*. The result (35)–(36) is valid for any choice of free energy functions $W^{(1)}$ and $W^{(2)}$ describing the elastic dielectric behaviors of the underlying matrix and particles. These include dielectrics with *odd* electroelastic coupling, such as piezoelectric materials, as well as dielectrics with *even* electroelastic coupling, or so called electrostrictive materials. In the next section, we work out specific results for a class of electrostrictive composites. The application of (35)–(36) to the odd-coupling case of piezoelectric composites will be reported elsewhere (Spinelli and Lopez-Pamies, submitted for publication).

(ii) *Geometry and spatial distribution of the particles*. The result (35)–(36) is also valid for any choice of one- and two-point correlation functions $p_0^{(2)}=c_0^{(2)}$ and $p_0^{(22)}$ describing the microstructure. The latter, again, contains fine information about the relative size, shape, and spatial distribution of the particles. Howbeit, it is remarkable that in spite of characterizing the *coupled* and *nonlinear* electroelastic properties of a wide class of elastic dielectric composites, the result (35)–(36)

does not depend on further information about the microstructure beyond $p_0^{(22)}$. What is more, the functional dependence of (35)–(36) on $p_0^{(22)}$ enters through the function $\nu(\boldsymbol{\xi})$, which is precisely the same geometrical object — a so-called H-measure (Tartar, 1990) — that appears in the context of analogous *linear* problems (Willis, 1981; Avellaneda and Milton, 1989).

(iii) *Interaction among particles*. By construction, the underlying microstructure associated with the effective free energy function (35)–(36) corresponds to a distribution of disconnected particles that interact in such a manner that their deformation gradient and electric field — irrespectively of the applied electromechanical loading, $\overline{\mathbf{F}}$ and $\overline{\mathbf{E}}$, and the value of the volume fraction of particles $c_0^{(2)}$ — are *uniform* and the *same* in each particle; a proof of this feature is provided in Appendix B within the context of a more general discussion on local fields. Such a special type of intraparticle fields is usually associated with microstructures that are extremal vis-á-vis *linear* properties (see, e.g., Milton and Kohn, 1988). For the *nonlinear* electroelastic properties at hand, the extremal character of the result (35)–(36) is yet to be proved or disproved.

(iv) *Mathematical tractability*. Eq. (35) is a first-order nonlinear pde of the Hamilton–Jacobi type. This class of pdes has appeared pervasively in a wide variety of fields, including control theory (Fleming and Rishel, 1975), geometrical optics (Born et al., 2003), and semi-classical quantum mechanics (Maslov and Fedoriuk, 1981). Accordingly, a substantial body of efficient numerical techniques has been and continues to be developed for solving this type of equations (Sethian, 1999). In spite of being nonlinear, Eq. (35) might also be solvable by analytical methods for especial cases (Lopez-Pamies et al., 2011b, 2013).

(v) *Realizability and the use of* (35)–(36) *as a constitutive theory*. The result (35)–(36) is exact for a specific class of two-phase particulate microstructures and hence it is realizable. What is more, in view of its applicability to arbitrary free energy functions $W^{(1)}$ and $W^{(2)}$ and arbitrary one-point $p_0^{(2)}$ and two-point $p_0^{(22)}$ correlation functions, the result (35)–(36) can be utilized more generally as a constitutive theory for two-phase elastic dielectrics with *any* particulate microstructure: for a given matrix constitutive behavior $W^{(1)}$, given particle constitutive behavior $W^{(2)}$, and given one- and two-point correlations $p_0^{(2)}$ and $p_0^{(22)}$, the result (35)–(36) provides a constitutive model for the macroscopic response of the elastic dielectric composite of interest.

4. Application to particle-filled ideal dielectrics

As a first application of the above-developed theory, we work out specific results for the basic case when the matrix material is an ideal elastic dielectric characterized by the free energy function

$$W^{(1)}(\mathbf{F},\mathbf{E})=\begin{cases}\dfrac{\mu}{2}[\mathbf{F}\cdot\mathbf{F}-3]-\dfrac{\varepsilon}{2}\mathbf{F}^{-T}\mathbf{E}\cdot\mathbf{F}^{-T}\mathbf{E} & \text{if } J=1\\ +\infty & \text{otherwise}\end{cases}. \tag{44}$$

The parameters μ and $\varepsilon=(1+\chi)\varepsilon_0$ denote, respectively, the shear modulus and permittivity of the material in its ground state. In the latter, χ stands for its electric susceptibility while the permittivity of vacuum is recalled to be given by $\varepsilon_0\approx 8.85\times 10^{-12}$ F/m. The elastic dielectric described by (44) is referred to as "ideal" in the sense that it is mechanically a Gaussian rubber whose polarization $\mathbf{p}$ remains linearly proportional to the applied Eulerian electric field $\mathbf{e}$ independently of the applied deformation: $\mathbf{p}=-\mathbf{F}\partial W^{(1)}(\mathbf{F},\mathbf{E})/\partial\mathbf{E}-\varepsilon_0\mathbf{F}^{-T}\mathbf{E}=\varepsilon_0\chi\mathbf{F}^{-T}\mathbf{E}=\varepsilon_0\chi\mathbf{e}$. In addition to its theoretical appeal and mathematical simplicity, the model (44) has been shown to describe reasonably well the electromechanical response of a variety of soft dielectrics over small-to-moderate ranges of deformations and large ranges of electric fields (see, e.g., Kofod et al., 2003; Wissler and Mazza, 2007).

Now, for the free energy function (44) the maximizing vector $\boldsymbol{\alpha}$ and minimizing scalar β in (35) can be determined explicitly. They read as

$$\boldsymbol{\alpha}=\frac{1}{\mu}\frac{\partial\overline{W}}{\partial\overline{\mathbf{F}}}\boldsymbol{\xi}-\overline{\mathbf{F}}\boldsymbol{\xi}+\frac{1}{\bar{J}\,\overline{\mathbf{F}}^{-T}\boldsymbol{\xi}\cdot\overline{\mathbf{F}}^{-T}\boldsymbol{\xi}}\overline{\mathbf{F}}^{-T}\boldsymbol{\xi}-\frac{\dfrac{\partial\overline{W}}{\partial\overline{\mathbf{F}}}\boldsymbol{\xi}\cdot\overline{\mathbf{F}}^{-T}\boldsymbol{\xi}}{\mu\overline{\mathbf{F}}^{-T}\boldsymbol{\xi}\cdot\overline{\mathbf{F}}^{-T}\boldsymbol{\xi}}\overline{\mathbf{F}}^{-T}\boldsymbol{\xi}+\frac{1}{\mu}\left(\frac{\partial\overline{W}}{\partial\overline{\mathbf{E}}}\cdot\boldsymbol{\xi}\right)\overline{\mathbf{F}}^{-T}\overline{\mathbf{E}}-\frac{\left(\dfrac{\partial\overline{W}}{\partial\overline{\mathbf{E}}}\cdot\boldsymbol{\xi}\right)\left(\overline{\mathbf{F}}^{-T}\overline{\mathbf{E}}\cdot\overline{\mathbf{F}}^{-T}\boldsymbol{\xi}\right)}{\mu\overline{\mathbf{F}}^{-T}\boldsymbol{\xi}\cdot\overline{\mathbf{F}}^{-T}\boldsymbol{\xi}}\overline{\mathbf{F}}^{-T}\boldsymbol{\xi} \tag{45}$$

and

$$\beta=\boldsymbol{\alpha}\cdot\overline{\mathbf{F}}^{-T}\overline{\mathbf{E}}-\frac{1}{\varepsilon\bar{J}^2\overline{\mathbf{F}}^{-T}\boldsymbol{\xi}\cdot\overline{\mathbf{F}}^{-T}\boldsymbol{\xi}}\left[\frac{\partial\overline{W}}{\partial\overline{\mathbf{E}}}\cdot\boldsymbol{\xi}+\varepsilon\bar{J}\,\overline{\mathbf{F}}^{-T}\overline{\mathbf{E}}\cdot\overline{\mathbf{F}}^{-T}\boldsymbol{\xi}\right], \tag{46}$$

where we recall that $\bar{J}=\det\overline{\mathbf{F}}$ and remark that the vector (45) satisfies the constraint $\det(\overline{\mathbf{F}}+\boldsymbol{\alpha}\otimes\boldsymbol{\xi})=1$, as dictated by the incompressibility of the matrix. After some lengthy but straightforward calculations, the explicit use of relations (45)–(46) in (35) allows to write the solution for the effective free energy function as

$$\overline{W}(\overline{\mathbf{F}},\overline{\mathbf{E}},c_0)=2\mu\overline{U}(\overline{\mathbf{F}},\overline{\mathbf{e}},c_0)+\frac{\mu}{2}[\overline{\mathbf{F}}\cdot\overline{\mathbf{F}}-3]-\frac{\varepsilon}{2}\overline{\mathbf{F}}^{-T}\overline{\mathbf{E}}\cdot\overline{\mathbf{F}}^{-T}\overline{\mathbf{E}}, \tag{47}$$

where $c_0 \doteq c_0^{(2)}$ has been introduced to ease notation, $\overline{\mathbf{e}} = \overline{\mathbf{F}}^{-T}\overline{\mathbf{E}}$ denotes the macroscopic electric field in the deformed configuration, and the function $\overline{U}$ is solution to the initial-value problem

$$\subset \frac{\partial \overline{U}}{\partial \subset} - \overline{U} - \left\langle \frac{\partial \overline{U}}{\partial \overline{\mathbf{F}}}\boldsymbol{\xi}\cdot\frac{\partial \overline{U}}{\partial \overline{\mathbf{F}}}\boldsymbol{\xi} - \frac{\left(\frac{\partial \overline{U}}{\partial \overline{\mathbf{F}}}\boldsymbol{\xi}\cdot\overline{\mathbf{F}}^{-T}\boldsymbol{\xi}\right)^2}{\overline{\mathbf{F}}^{-T}\boldsymbol{\xi}\cdot\overline{\mathbf{F}}^{-T}\boldsymbol{\xi}} - \frac{\mu}{\varepsilon}\frac{\left(\frac{\partial \overline{U}}{\partial \overline{\mathbf{e}}}\cdot\overline{\mathbf{F}}^{-T}\boldsymbol{\xi}\right)^2}{\bar{J}^2\overline{\mathbf{F}}^{-T}\boldsymbol{\xi}\cdot\overline{\mathbf{F}}^{-T}\boldsymbol{\xi}} + \frac{(1-\bar{J})}{\bar{J}^2\overline{\mathbf{F}}^{-T}\boldsymbol{\xi}\cdot\overline{\mathbf{F}}^{-T}\boldsymbol{\xi}} \times \left[\frac{(\bar{J}-1)}{4} + \bar{J}\frac{\partial \overline{U}}{\partial \overline{\mathbf{F}}}\boldsymbol{\xi}\cdot\overline{\mathbf{F}}^{-T}\boldsymbol{\xi} + \frac{(\bar{J}-1)\varepsilon}{4\mu}(\overline{\mathbf{e}}\cdot\overline{\mathbf{F}}^{-T}\boldsymbol{\xi})^2 + \left(\overline{\mathbf{e}}\cdot\overline{\mathbf{F}}^{-T}\boldsymbol{\xi}\right)\frac{\partial \overline{U}}{\partial \overline{\mathbf{e}}}\cdot\overline{\mathbf{F}}^{-T}\boldsymbol{\xi}\right]\right\rangle = 0 \tag{48}$$

with

$$\overline{U}(\overline{\mathbf{F}},\overline{\mathbf{e}},1) = \frac{1}{2\mu}W^{(2)}\left(\overline{\mathbf{F}},\overline{\mathbf{F}}^T\overline{\mathbf{e}}\right) - \frac{1}{4}\left[\overline{\mathbf{F}}\cdot\overline{\mathbf{F}}-3\right] + \frac{\varepsilon}{4\mu}\overline{\mathbf{e}}\cdot\overline{\mathbf{e}}. \tag{49}$$

The computation of the effective free energy function (47) of particle-filled ideal dielectrics amounts thus to solving the first-order pde (48) with *quadratic* nonlinearity. We emphasize that the result (47) with (48)–(49) is valid for any free energy function $W^{(2)}$ of choice. Accordingly, it allows to consider a broad range of elastic dielectric behaviors for the particles. These include limiting behaviors of practical interest, such as particles that are mechanically vacuous or rigid, as well as particles with dielectric responses that grow linearly or saturate for large values of the applied electric field.

4.1. Ideal dielectric particles

In the sequel, we focus on particles that are ideal elastic dielectrics themselves. Similar to (44), we write their free energy function as

$$W^{(2)}(\mathbf{F},\mathbf{E}) = \begin{cases} \frac{\mu_p}{2}[\mathbf{F}\cdot\mathbf{F}-3] - \frac{\varepsilon_p}{2}\mathbf{F}^{-T}\mathbf{E}\cdot\mathbf{F}^{-T}\mathbf{E} & \text{if } J=1 \\ +\infty & \text{otherwise} \end{cases}, \tag{50}$$

where μ_p and $\varepsilon_p = (1+\chi_p)\varepsilon_0$ stand for their shear modulus and permittivity in the ground state, while χ_p denotes their electric susceptibility. We point out that the model (50) includes extremal behaviors of notable relevance in applications such as rigid conducting particles, corresponding to the choice $\mu_p \to \infty$ and $\varepsilon_p \to \infty$, and liquid conducting particles, corresponding to $\mu_p \to 0$ and $\varepsilon_p \to \infty$.

For the specific class of particle behaviors (50), it is a simple matter to show that the effective free energy function (47) reduces further to

$$\overline{W}(\overline{\mathbf{F}},\overline{\mathbf{E}},c_0) = \begin{cases} 2\mu\overline{U}(\overline{\mathbf{F}},\overline{\mathbf{e}},c_0) + \frac{\mu}{2}\left[\overline{\mathbf{F}}\cdot\overline{\mathbf{F}}-3\right] - \frac{\varepsilon}{2}\overline{\mathbf{F}}^{-T}\overline{\mathbf{E}}\cdot\overline{\mathbf{F}}^{-T}\overline{\mathbf{E}} & \text{if } \bar{J}=1 \\ +\infty & \text{otherwise} \end{cases} \tag{51}$$

where now the function $\overline{U}$ is solution to the simpler initial-value problem

$$\subset \frac{\partial \overline{U}}{\partial \subset} - \overline{U} - \left\langle \frac{\partial \overline{U}}{\partial \overline{\mathbf{F}}}\boldsymbol{\xi}\cdot\frac{\partial \overline{U}}{\partial \overline{\mathbf{F}}}\boldsymbol{\xi} - \frac{\left(\frac{\partial \overline{U}}{\partial \overline{\mathbf{F}}}\boldsymbol{\xi}\cdot\overline{\mathbf{F}}^{-T}\boldsymbol{\xi}\right)^2}{\overline{\mathbf{F}}^{-T}\boldsymbol{\xi}\cdot\overline{\mathbf{F}}^{-T}\boldsymbol{\xi}} - \frac{\mu}{\varepsilon}\frac{\left(\frac{\partial \overline{U}}{\partial \overline{\mathbf{e}}}\cdot\overline{\mathbf{F}}^{-T}\boldsymbol{\xi}\right)^2}{\overline{\mathbf{F}}^{-T}\boldsymbol{\xi}\cdot\overline{\mathbf{F}}^{-T}\boldsymbol{\xi}}\right\rangle = 0 \tag{52}$$

with

$$\overline{U}(\overline{\mathbf{F}},\overline{\mathbf{e}},1) = \frac{1}{4}\left(\frac{\mu_p}{\mu}-1\right)\left[\overline{\mathbf{F}}\cdot\overline{\mathbf{F}}-3\right] + \frac{\varepsilon-\varepsilon_p}{4\mu}\overline{\mathbf{e}}\cdot\overline{\mathbf{e}}. \tag{53}$$

As expected, the *local* incompressibility of both the matrix (44) and particles (50) imply that the composite itself is incompressible and thus obeys the *macroscopic* kinematical constraint $C(\overline{\mathbf{F}}) = \det\overline{\mathbf{F}} - 1 = 0$. The result (51) is still fairly general in that it applies to broad classes of microstructures, as characterized by the volume fraction of particles c_0 and their two-point correlation function via the integral operator $\langle\cdot\rangle$ in (52). Two classes of particulate microstructures of current experimental interest (see, e.g., Razzaghi Kashani et al., 2010) are those comprised of (roughly) spherical particles of the same size that are distributed (i) isotropically or (ii) in chain-like formations. Fig. 3 depicts schematics of such microstructures. For demonstration purposes and later use, we spell out next their mathematical description within the context of the result (51).

4.1.1. Isotropic distributions of spherical particles

For particulate microstructures made up of spherical particles whose centers are distributed randomly with isotropic symmetry, the microstructural function $(42)_1$ can be determined explicitly (Willis, 1981). The result reads simply as

$$\nu(\boldsymbol{\xi}) = \frac{1}{4\pi}, \tag{54}$$

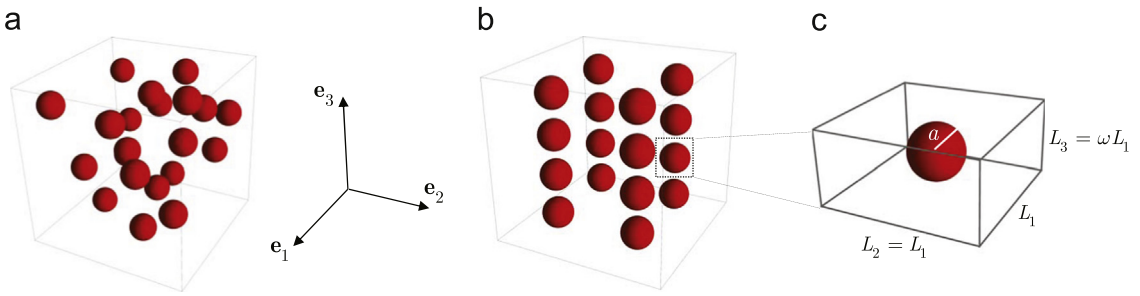

Fig. 3. Schematics of (a) isotropic and (b) chain-like distributions of spherical particles. Chain-like distributions are modeled here as periodic arrays of spherical particles where the repeating unit cell (c) is a rectangular prism with two equal sides — of lengths $L_1, L_2 = L_1, L_3$ — containing a single particle — of radius a — located at its center; the parameter $\omega = L_3/L_1$ describes the aspect ratio of the unit cell.

and so the pde (52) for the function $\overline{U}$ specializes in this case to

$$c\frac{\partial \overline{U}}{\partial c} - \overline{U} - \frac{1}{4\pi}\int_{|\boldsymbol{\xi}|=1}\left[\frac{\partial \overline{U}}{\partial \overline{\mathbf{F}}}\boldsymbol{\xi}\cdot\frac{\partial \overline{U}}{\partial \overline{\mathbf{F}}}\boldsymbol{\xi} - \frac{\left(\frac{\partial \overline{U}}{\partial \overline{\mathbf{F}}}\boldsymbol{\xi}\cdot\overline{\mathbf{F}}^{-T}\boldsymbol{\xi}\right)^2}{\overline{\mathbf{F}}^{-T}\boldsymbol{\xi}\cdot\overline{\mathbf{F}}^{-T}\boldsymbol{\xi}} - \frac{\mu}{\varepsilon}\frac{\left(\frac{\partial \overline{U}}{\partial \overline{\mathbf{e}}}\cdot\overline{\mathbf{F}}^{-T}\boldsymbol{\xi}\right)^2}{\overline{\mathbf{F}}^{-T}\boldsymbol{\xi}\cdot\overline{\mathbf{F}}^{-T}\boldsymbol{\xi}}\right]d\boldsymbol{\xi} = 0. \tag{55}$$

4.1.2. Chain-like distributions of spherical particles

As illustrated in Fig. 3(b) and (c), chain-like distributions of spherical particles are idealized here as periodic microstructures where the repeating unit cell is comprised of a rectangular prism with two equal sides containing a single spherical particle located at its center. We denote the lengths of the sides of the prism by $L_1, L_2 = L_1, L_3$, and the length of the radius of the particle by a. The associated lattice over which the unit cell is repeated is given by $\mathcal{R} = \{\mathbf{Y} : \mathbf{Y} = L_1 n_1\,\mathbf{e}_1 + L_1 n_2\,\mathbf{e}_2 + L_3 n_3\,\mathbf{e}_3, \quad n_i \in \mathbb{Z}\}$, where $\mathbf{e}_1, \mathbf{e}_2, \mathbf{e}_3$ are the Cartesian laboratory axes, chosen here to coincide with the principal axes of the unit cell. After carrying out the required Fourier transform $(38)_2$ and calculation of the reciprocal lattice (39)–(40), the function $(38)_1$ associated with this microstructure takes the explicit form

$$\nu(\boldsymbol{\xi}) = \sum_{\mathbf{k}\in\mathcal{R}^*-\{\mathbf{0}\}} \frac{9(\sin\eta - \eta\cos\eta)^2 c_0}{\eta^6(1-c_0)}\,\delta\left(\boldsymbol{\xi} - \frac{\mathbf{k}}{|\mathbf{k}|}\right) \quad \text{with } \eta = a|\mathbf{k}| \tag{56}$$

and

$$\mathcal{R}^* = \left\{\mathbf{k} : \mathbf{k} = \frac{2\pi}{L_1}n_1\,\mathbf{e}_1 + \frac{2\pi}{L_1}n_2\,\mathbf{e}_2 + \frac{2\pi}{L_3}n_3\,\mathbf{e}_3, \quad n_i \in \mathbb{Z}\right\}. \tag{57}$$

For this class of chain-like distributions of spherical particles, the pde (52) for the function $\overline{U}$ specializes thus to

$$c\frac{\partial \overline{U}}{\partial c} - \overline{U} - \sum_{\substack{\mathbf{k}\in\mathcal{R}^*-\{\mathbf{0}\}\\ \boldsymbol{\xi}=\mathbf{k}/|\mathbf{k}|}} \frac{9(\sin\eta - \eta\cos\eta)^2 c_0}{\eta^6(1-c_0)}\left[\frac{\partial \overline{U}}{\partial \overline{\mathbf{F}}}\boldsymbol{\xi}\cdot\frac{\partial \overline{U}}{\partial \overline{\mathbf{F}}}\boldsymbol{\xi} - \frac{\left(\frac{\partial \overline{U}}{\partial \overline{\mathbf{F}}}\boldsymbol{\xi}\cdot\overline{\mathbf{F}}^{-T}\boldsymbol{\xi}\right)^2}{\overline{\mathbf{F}}^{-T}\boldsymbol{\xi}\cdot\overline{\mathbf{F}}^{-T}\boldsymbol{\xi}} - \frac{\mu}{\varepsilon}\frac{\left(\frac{\partial \overline{U}}{\partial \overline{\mathbf{e}}}\cdot\overline{\mathbf{F}}^{-T}\boldsymbol{\xi}\right)^2}{\overline{\mathbf{F}}^{-T}\boldsymbol{\xi}\cdot\overline{\mathbf{F}}^{-T}\boldsymbol{\xi}}\right] = 0. \tag{58}$$

5. Sample results

A common experiment to characterize the performance of deformable dielectrics consists in exposing them to a uniaxial electric field while they are biaxially stretched in the transverse direction. In practice, this is typically accomplished by sandwiching a thin layer of stretched dielectric in between two compliant electrodes connected to a battery[8] (see, e.g., Section 2.25 in Stratton, 1941; Pelrine et al., 1998, 2000). In the sequel, we consider such type of loading conditions on the particle-filled ideal dielectrics described in the forgoing section, with both, isotropic and chain-like distributions of spherical particles. In addition to illustrating the usage of the theory within the context of a simple yet experimentally relevant problem, we aim at shedding light on how the addition of filler particles can improve the performance of deformable dielectrics.

[8] For such a configuration, the electric field is roughly uniform (macroscopically) within the dielectric and zero outside of it.

We begin by considering macroscopic electromechanical loadings of the form

$$\overline{F}_{ij}=\begin{bmatrix}\overline{\lambda} & 0 & 0\\ 0 & \overline{\lambda} & 0\\ 0 & 0 & \overline{\lambda}^{-2}\end{bmatrix},\quad \overline{E}_i=\begin{bmatrix}0\\0\\\overline{E}\end{bmatrix}, \tag{59}$$

where $\overline{\lambda}>0$ and $\overline{E}$ are loading parameters denoting the applied biaxial stretch and Lagrangian electric field; throughout this section, the components of any tensorial quantity are referred to the Cartesian laboratory axes $\mathbf{e}_1$, $\mathbf{e}_2$, $\mathbf{e}_3$ depicted in Fig. 3. From the overall orthotropy of either (isotropic or chain-like) distribution of particles, it follows that the resulting macroscopic first Piola–Kirchhoff stress and Lagrangian electric displacement are of the form

$$\overline{S}_{ij}=\begin{bmatrix}\overline{S} & 0 & 0\\ 0 & \overline{S} & 0\\ 0 & 0 & 0\end{bmatrix},\quad \overline{D}_i=\begin{bmatrix}0\\0\\\overline{D}\end{bmatrix}, \tag{60}$$

where we have selected the arbitrary pressure associated with the incompressibility constraint, $C(\overline{\mathbf{F}})=\det\overline{\mathbf{F}}-1=0$, of the composites under study here to be such that the normal stress in the direction of the applied electric field vanishes, $\overline{S}_{33}=0$, in accordance with the experimental boundary conditions.

In terms of the loading parameters $\overline{\lambda}$ and $\overline{E}$, the non-trivial components of the stress $(60)_1$ and electric displacement $(60)_2$ are given by

$$\overline{S}=\frac{1}{2}\frac{\partial\tilde{W}}{\partial\overline{\lambda}}(\overline{\lambda},\overline{E},c_0),\quad \overline{D}=-\frac{\partial\tilde{W}}{\partial\overline{E}}(\overline{\lambda},\overline{E},c_0), \tag{61}$$

where $\tilde{W}(\overline{\lambda},\overline{E},c_0)=\overline{W}(\overline{\mathbf{F}},\overline{\mathbf{E}},c_0)$ stands for the finite branch of the effective free energy function (51). From (51) and (52)–(53), it follows in particular that

$$\tilde{W}(\overline{\lambda},\overline{E},c_0)=2\mu\tilde{U}(\overline{\lambda},\overline{e},c_0)+\frac{\mu}{2}\left[2\overline{\lambda}^2+\overline{\lambda}^{-4}-3\right]-\frac{\varepsilon}{2}\overline{\lambda}^4\overline{E}^2, \tag{62}$$

where $\overline{e}=\overline{\lambda}^2\,\overline{E}$ denotes the macroscopic electric field in the deformed configuration and the function $\tilde{U}$ is solution to the pde

$$c\frac{\partial\tilde{U}}{\partial c}-\tilde{U}-g_1(\overline{\lambda})\left(\frac{\partial\tilde{U}}{\partial\overline{\lambda}}\right)^2-\frac{\mu}{\varepsilon}g_2(\overline{\lambda})\left(\frac{\partial\tilde{U}}{\partial\overline{e}}\right)^2=0 \tag{63}$$

with initial condition

$$\tilde{U}(\overline{\lambda},\overline{e},1)=\frac{1}{4}\left(\frac{\mu_p}{\mu}-1\right)\left[2\overline{\lambda}^2+\overline{\lambda}^{-4}-3\right]+\frac{\varepsilon-\varepsilon_p}{4\mu}\,\overline{e}^2. \tag{64}$$

The coefficients g_1 and g_2 in (63) are functions of the stretch $\overline{\lambda}$ that depend on the microstructure. For *isotropic* distributions of spherical particles, they are given by

$$g_1(\overline{\lambda})=\frac{(2\overline{\lambda}^6+1)\overline{\lambda}^6}{12(\overline{\lambda}^6-1)^2}-\frac{\overline{\lambda}^{12}\ln\left[\overline{\lambda}^{-3}+\sqrt{\overline{\lambda}^{-6}-1}\right]}{4(1-\overline{\lambda}^6)^{5/2}}\quad\text{and}\quad g_2(\overline{\lambda})=\frac{\overline{\lambda}^6}{1-\overline{\lambda}^6}-\frac{\ln\left[\overline{\lambda}^{-3}+\sqrt{\overline{\lambda}^{-6}-1}\right]}{(\overline{\lambda}^{-6}-1)^{3/2}\overline{\lambda}^3}. \tag{65}$$

For *chain-like* distributions of spherical particles, on the other hand, they take the form

$$g_1(\overline{\lambda})=\frac{c_0}{1-c_0}\sum_{\mathrm{p}=-\infty}^{+\infty}\sum_{\mathrm{q}=-\infty}^{+\infty}\sum_{\mathrm{r}=-\infty}^{+\infty}{}_{-\{\mathrm{p}=\mathrm{q}=\mathrm{r}=0\}}\frac{\overline{\lambda}^6\omega^2\mathrm{r}^2(\mathrm{p}^2+\mathrm{q}^2)\left[\frac{9}{\eta^6}(\sin\eta-\eta\cos\eta)^2\right]}{4(\omega^2(\mathrm{p}^2+\mathrm{q}^2)+\mathrm{r}^2)(\omega^2(\mathrm{p}^2+\mathrm{q}^2)+\overline{\lambda}^6\mathrm{r}^2)} \tag{66}$$

and

$$g_2(\overline{\lambda})=-\frac{c_0}{1-c_0}\sum_{\mathrm{p}=-\infty}^{+\infty}\sum_{\mathrm{q}=-\infty}^{+\infty}\sum_{\mathrm{r}=-\infty}^{+\infty}{}_{-\{\mathrm{p}=\mathrm{q}=\mathrm{r}=0\}}\frac{\overline{\lambda}^6\mathrm{r}^2\left[\frac{9}{\eta^6}(\sin\eta-\eta\cos\eta)^2\right]}{\omega^2(\mathrm{p}^2+\mathrm{q}^2)+\overline{\lambda}^6\mathrm{r}^2}, \tag{67}$$

where $\eta=6^{1/3}\pi^{2/3}c_0^{1/3}\omega^{1/3}\sqrt{\mathrm{p}^2+\mathrm{q}^2+\mathrm{r}^2/\omega^2}$ and $\omega=L_3/L_1$ is the aspect ratio of the unit cell. The computation of the macroscopic response — as characterized by expressions (61) with (62) — of either type of elastic dielectric composite (with isotropic or chain-like microstructures) amounts thus to solving equation (63), a first-order pde in two variables with quadratic nonlinearity, subject to the initial condition (64).

5.1. Classical limit of small deformations and small electric fields

In the limit of small deformations and small electric fields as $\overline{\lambda}\to 1$ and $\overline{E}\to 0$, the initial-value problem (63)–(64) admits an explicit solution and so the effective free energy function (62) can be written in closed form. The result reads as

$$\tilde{W}(\overline{\lambda},\overline{E},c_0)=\frac{1}{2}\mathcal{L}(c_0)(\overline{\lambda}-1)^2-\frac{1}{2}\mathcal{B}(c_0)\overline{E}^2-\mathcal{M}(c_0)(\overline{\lambda}-1)\overline{E}^2 \tag{68}$$

to order[9] $O(2)$ in the strain measure $(\overline{\lambda}-1)$ and electric field $\overline{E}$, where

$$\begin{aligned}
\mathcal{L}(c_0)&=12\mu+\frac{12c_0(\mu-\mu_p)}{(2a_1-1)\mu-2a_1\mu_p}\mu,\\
\mathcal{B}(c_0)&=\varepsilon-\frac{c_0\,(\varepsilon-\varepsilon_p)}{a_2\varepsilon-a_2\varepsilon_p+\varepsilon}\,\varepsilon,\\
\mathcal{M}(c_0)&=2\varepsilon-2\frac{c_0\,(\varepsilon-\varepsilon_p)}{a_2\varepsilon-a_2\varepsilon_p+\varepsilon}\,\varepsilon-\frac{2a_1c_0(\varepsilon-\varepsilon_p)^2\left[(a_1-1)\mu-a_1\mu_p\right]}{\left[(2a_1-1)\mu-2a_1\mu_p\right](a_2\varepsilon-a_2\varepsilon_p+\varepsilon)^2}\,\varepsilon.
\end{aligned} \tag{69}$$

In these coefficients, we have made use of the notation

$$a_1=6(1-c_0)g_1(1)\quad\text{and}\quad a_2=(1-c_0)g_2(1), \tag{70}$$

where, again, the functions g_1 and g_2 are given by expressions (65) and (66)–(67) for isotropic and chain-like distributions of spherical particles, respectively. Accordingly, for isotropic distributions of spherical particles

$$g_1(1)=\frac{1}{30}\quad\text{and}\quad g_2(1)=-\frac{1}{3}, \tag{71}$$

whereas for chain-like distributions of spherical particles

$$g_1(1)=\frac{c_0}{1-c_0}\sum_{\mathfrak{p}=-\infty}^{+\infty}\sum_{\mathfrak{q}=-\infty}^{+\infty}\sum_{\mathfrak{r}=-\infty}^{+\infty}{}'\,\frac{\omega^2\mathfrak{r}^2(\mathfrak{p}^2+\mathfrak{q}^2)\left[\frac{9}{\eta^6}(\sin\eta-\eta\cos\eta)^2\right]}{4(\omega^2(\mathfrak{p}^2+\mathfrak{q}^2)+\mathfrak{r}^2)^2} \tag{72}$$

and

$$g_2(1)=-\frac{c_0}{1-c_0}\sum_{\mathfrak{p}=-\infty}^{+\infty}\sum_{\mathfrak{q}=-\infty}^{+\infty}\sum_{\mathfrak{r}=-\infty}^{+\infty}{}'\,\frac{\mathfrak{r}^2\left[\frac{9}{\eta^6}(\sin\eta-\eta\cos\eta)^2\right]}{\omega^2(\mathfrak{p}^2+\mathfrak{q}^2)+\mathfrak{r}^2} \tag{73}$$

with $\eta=6^{1/3}\pi^{2/3}c_0^{1/3}\omega^{1/3}\sqrt{\mathfrak{p}^2+\mathfrak{q}^2+\mathfrak{r}^2/\omega^2}$.

While limited because of its asymptotic nature, the analytical result (68) is still fairly general in that it allows to examine the effects that loading conditions ($\overline{\lambda}$ and $\overline{E}$), particle stiffness and permittivity (μ_p and ε_p), and particle volume fraction and spatial distribution (c_0 and ω) have on the performance of particle-filled deformable dielectrics. A full parametric study of the result (68) is beyond the illustrative purposes of this section. Thus, for conciseness, we restrict attention to the experimentally standard case when no mechanical tractions are applied so that the deformation is solely due to the applied electric field. Under this type of loading conditions, the primary quantity of interest is the "actuation" strain in the transverse direction to the electric field. Making use of the result (68) in the zero-traction condition $\overline{S}=1/2\,\partial\tilde{W}(\overline{\lambda},\overline{E},c_0)/\partial\overline{\lambda}=0$ leads to the following formula for such an electrically induced strain:

$$\overline{\in}\,\overset{\bullet}{=}\,\overline{\lambda}-1=\frac{\mathcal{M}(c_0)}{\mathcal{L}(c_0)}\,\overline{E}^2. \tag{74}$$

In the absence of particles ($c_0=0$), the actuation strain is given by the matrix actuation strain $\overline{\in}_{mat}\,\overset{\bullet}{=}\,\overline{\lambda}_{mat}-1=\varepsilon/6\mu\overline{E}^2$, and so the ratio

$$\frac{\overline{\in}}{\overline{\in}_{mat}}=\frac{6\mu\mathcal{M}(c_0)}{\varepsilon\mathcal{L}(c_0)}=\frac{\left(2a_1-1-2a_1\frac{\mu_p}{\mu}\right)\left(a_2-c_0+1+(c_0-a_2)\frac{\varepsilon_p}{\varepsilon}\right)}{\left(a_2+1-a_2\frac{\varepsilon_p}{\varepsilon}\right)\left(2a_1+c_0-1-(2a_1+c_0)\frac{\mu_p}{\mu}\right)}-\frac{a_1c_0\left(a_1-1-a_1\frac{\mu_p}{\mu}\right)\left(1-\frac{\varepsilon_p}{\varepsilon}\right)^2}{\left(a_2+1-a_2\frac{\varepsilon_p}{\varepsilon}\right)^2\left(2a_1+c_0-1-(2a_1+c_0)\frac{\mu_p}{\mu}\right)} \tag{75}$$

[9] Note that the power series result (68) is asymptotically exact for electric fields $\overline{E}$ of $O(\sqrt{\delta})$ when the strains $(\overline{\lambda}-1)$ are of $O(\delta)$.

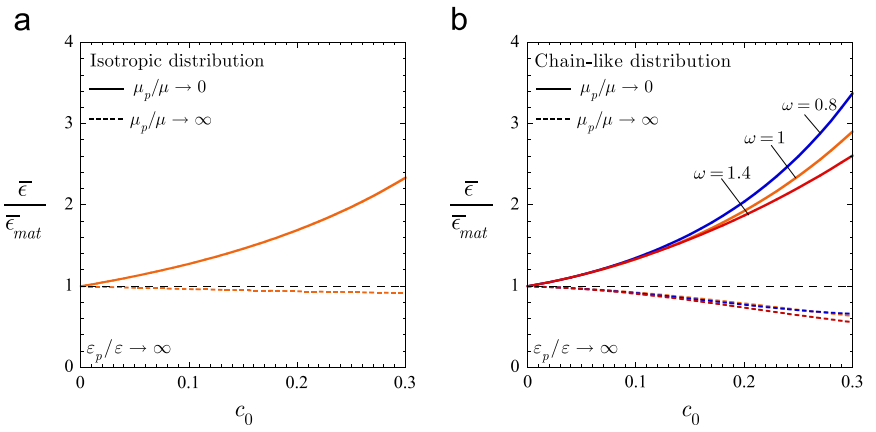

Fig. 4. Actuation strain $\in$ of particle-filled ideal dielectrics, normalized by the actuation strain $\in_m$ at of the underlying matrix, with (a) isotropic and (b) chain-like distributions of conducting ($\varepsilon_p/\varepsilon \to \infty$) spherical particles, as determined by the explicit expression (75). Results are shown for rigid ($\mu_p/\mu \to \infty$) and liquid ($\mu_p/\mu \to 0$) particles in terms of their volume fraction c_0. The results in (b) are for three decreasing values of the unit-cell aspect ratio, $\omega = 1.4, 1, 0.8$, corresponding to chains with increasingly closer particle packing in the direction of the applied electric field.

provides insight into how the addition of particles affects the electrostriction of deformable dielectrics. Direct inspection reveals that the ratio (75) depends on the electroelastic properties of the matrix and particles only through the combinations μ_p/μ and $\varepsilon_p/\varepsilon$, and that, as expected, it decreases with increasing values of μ_p/μ while it increases with increasing $\varepsilon_p/\varepsilon$. The dependence on the microstructure through the volume fraction c_0 and spatial distribution ω of the particles is not monotonic and thus more intricate.

To gain more quantitative understanding, Fig. 4 shows results for the normalized actuation strain (75) for the extremal cases[10] of dielectrics filled with infinite-permittivity, or equivalently, conducting particles, $\varepsilon_p/\varepsilon \to \infty$, that mechanically are either rigid, $\mu_p/\mu \to \infty$, or "liquid" with zero shear modulus $\mu_p/\mu \to 0$. The data is plotted in terms of the particle volume fraction c_0 for (a) isotropic and (b) chain-like distributions of the particles. The results in part (b) are for three decreasing values of the unit-cell aspect ratio $\omega = 1.4$, 1, 0.8, which correspond to increasingly closer packing of the particles in the direction of the applied electric field; see Fig. 3(c).

An immediate observation from Fig. 4(a) is that the addition of liquid conducting particles leads to a significant enhancement of the actuation strain ($\overline{\epsilon}/\overline{\epsilon}_{mat} > 1$). The opposite is true ($\overline{\epsilon}/\overline{\epsilon}_{mat} < 1$) when the conducting particles that are added are mechanically rigid, although the quantitative reduction of the actuation strain is not quite as significant. Physically, these two behaviors can be understood as follows. Independently of their mechanical behavior, the addition of conducting particles enhances the overall electrostriction of the material because it increases the overall permittivity. Now, for the case when the particles are liquid, the overall electrostriction of the material is enhanced even further because the addition of particles — being mechanically of zero shear stiffness — also increases the overall deformability. For the case when the particles are rigid, by contrast, the overall electrostriction is reduced due to the decrease in overall deformability that ensues from the addition of stiff particles. In this latter case, the decrease in deformability due to mechanical stiffening turns out to outweigh the increase in permittivity and so the actuation strains of dielectrics filled with rigid conducting particles turn out to be smaller than those of the same dielectrics without particles.

The same above conclusions can be drawn from Fig. 4(b). Additionally, the results in this figure indicate that the actuation strains are larger for liquid particles when the particles are distributed anisotropically in chain-like formations instead of isotropically. And, in particular, that this enhancement in electrostriction improves when the particles in the chains are closer to each other in the direction of the applied electric field. When the particles are mechanically rigid, on the other hand, chain-like distributions lead to larger reductions of the actuation strains than isotropic distributions. Placing the particles closer to each other in the direction of the applied electric field does not significantly alter this reduction in electrostriction, at least for the range of particle volume fractions $c_0 \in [0, 0.3]$ considered here.

5.2. *Results for finite deformations and finite electric fields*

For arbitrarily large stretches $\overline{\lambda}$ and electric fields $\overline{E}$, the initial-value problem (63)–(64) and thus the effective free energy function (62) may plausibly admit a closed-form solution. Here, at any rate, we shall be content with reporting numerical solutions for it. Continuing the focus of the preceding subsection, Fig. 5 shows results for the macroscopic stretch $\overline{\lambda}$ induced by the application of an electric field $\overline{E}/\sqrt{\mu/\varepsilon}$ when no mechanical tractions are applied so that $\overline{S} = 1/2\, \partial \tilde{W}(\overline{\lambda}, \overline{E}, c_0)/\partial \overline{\lambda} = 0$. Much like the results in Fig. 4, the results in Fig. 5 correspond to ideal dielectrics filled with spherical conducting particles,

[10] When compared to elastomers, many ceramics and metals can be considered to be of infinite permittivity and of infinite shear modulus. On the other hand, many fluids and eutectic alloys (e.g., Galinstan) can be considered to be also of infinite permittivity but of zero shear modulus.

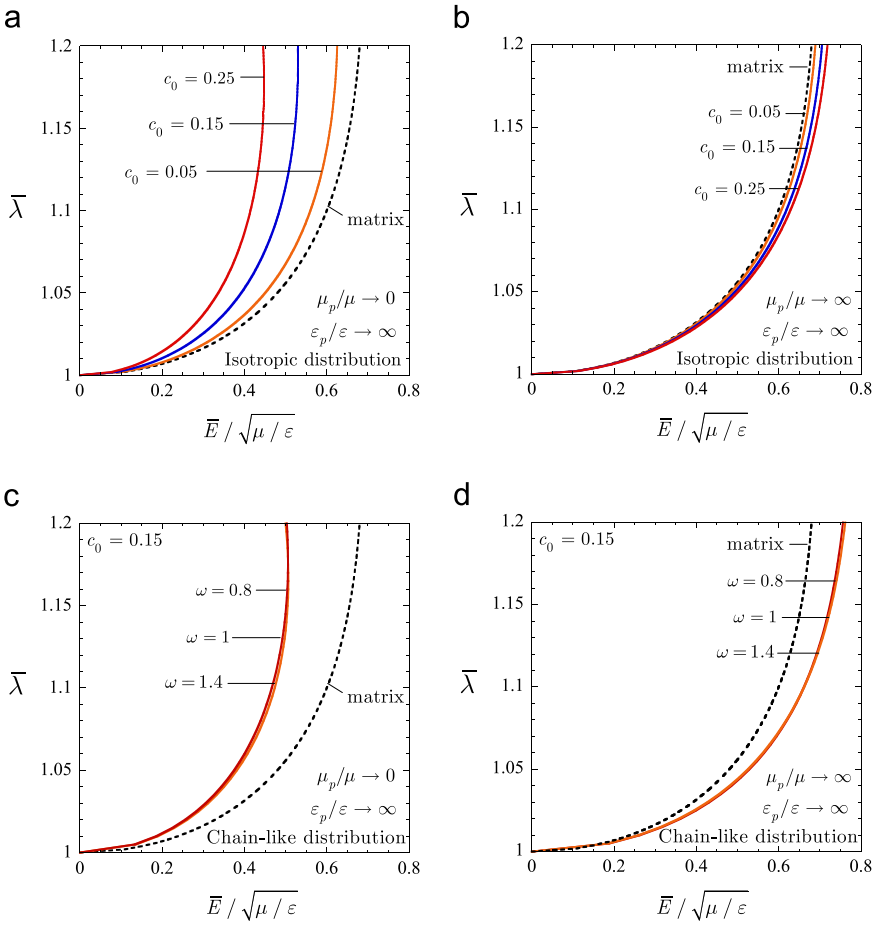

Fig. 5. Actuation stretch $\overline{\lambda}$ of particle-filled ideal dielectrics with (a, b) isotropic and (c, d) chain-like distributions of conducting ($\varepsilon_p/\varepsilon \to \infty$) spherical particles. Results are shown in terms of the applied electric field $\overline{E}/\sqrt{\mu/\varepsilon}$ for rigid ($\mu_p/\mu \to \infty$) and liquid ($\mu_p/\mu \to 0$) particles. The results in (a, b) are for volume fractions $c_0 = 0.05, 0.15, 0.25$, while those in (c, d) are for $c_0 = 0.15$ and three decreasing values of the unit-cell aspect ratio, $\omega = 1.4, 1, 0.8$, corresponding to chains with increasingly closer particle packing in the direction of the applied electric field.

$p/\varepsilon \to \infty$, that mechanically are either rigid, $\mu_p/\mu \to \infty$, or liquid, $\mu_p/\mu \to 0$, and that are distributed isotropically (a, b) or in chain-like formations (c, d).

In line with the trends observed in the regime of small deformations and small electric fields, it is plain from Fig. 5 that the addition of liquid conducting particles — irrespectively of their spatial distribution — enhances significantly the actuation stretch of ideal dielectrics and that this enhancement increases with the volume fraction of particles c_0. By contrast, the addition of rigid conducting particles results in actuation stretches that are smaller than those experienced by the matrix material without particles (shown by the dashed line in the plots). Further, when the particles are liquid (rigid) and are distributed in chain-like formations, the actuation stretches are larger (smaller) than when they are merely distributed randomly with isotropic symmetry. Interestingly, sizable variations of the distance between the particles in the chains in the direction of the applied electric field, as characterized by the values of unit-cell aspect ratios $\omega = 1.4$, 1, 0.8, do not significantly affect the resulting actuation stretches, even for the relative high value of particle volume fraction $c_0 = 0.15$ considered in parts (c) and (d) of the figure.

In short, the above sample results have illustrated that in spite of accounting for fine microscopic information the proposed theory (35)–(36) is indeed computationally tractable. And hence that it provides an efficient analytical tool to gain quantitative insight into how the underlying microscopic behavior affects the macroscopic behavior of elastic dielectric composites at finite deformations and finite electric fields. As per the results themselves, they have revealed *inter alia* that the addition of high-permittivity particles that are mechanically softer than the matrix material leads to significantly larger electrostrictive deformations. And that the addition of high-permittivity particles that, on the other hand, are mechanically stiffer than the matrix material leads to smaller electrostrictive deformations. It would be interesting to explore these theoretical results experimentally. More thorough analyses of the electromechanical performance of particle-filled dielectrics with different constitutive behaviors for the matrix and particles, as well as with different particle sizes, shapes, and spatial distributions will be reported in future work with the objective of guiding the optimal design of this remarkable class of electroactive materials.

6. Final remarks

In soft elastic dielectric composites such as filled elastomers, the portion of material surrounding the filler particles — often referred to as "bound rubber" or more generally as interphase — can exhibit mechanical and dielectric behaviors markedly different from those of the elastomeric matrix in the bulk (see, e.g., Leblanc, 2010; Roy et al., 2005). Roughly speaking, this is because the anchoring of the polymeric chains of the matrix onto the filler particles forces the chains into conformations that are very different from those in the bulk, hence resulting in very different properties. In addition, and perhaps more importantly, such interphases may also contain space charges (see, e.g., Lewis, 2004). These underlying interphasial features are suspected to play a significant (if not dominant) role on the resulting macroscopic response, especially when the filler particles are submicrometer in size. It would be of great theoretical and practical value to extend the framework presented in this paper to account for such interphasial phenomena.

We conclude by remarking that the techniques *per se* developed in this work can be utilized to model a number of other classes of active material systems. For instance, making use of the well-known mathematical analogy between electroelastostatics and magnetoelastostatics, the result (35)–(36) — as well as its ($\mathbf{F}$, $\mathbf{D}$)-version (106)–(107) — can be utilized *mutatis mutandis* to model magnetorheological elastomers (see, e.g., Danas et al., 2012).

Acknowledgments

Support for this work by the National Science Foundation through CAREER Grant CMMI–1219336 is gratefully acknowledged.

Appendix A. The relation between $\nu(\boldsymbol{\xi})$ and the two-point correlation $p_0^{(22)}$

The microstructural information contained in the function $\nu(\boldsymbol{\xi})$ is decrypted here by analyzing the behavior of the result (35)–(36) in the limit of weak inhomogeneity as $\Delta W = W^{(2)} - W^{(1)} \to 0$. In order to minimize the calculations involved, attention is restricted to the weak-inhomogeneity limit within the linearly elastic regime of small deformations $\overline{\mathbf{F}} \to \mathbf{I}$ in the absence of electric fields $\overline{\mathbf{E}} = \mathbf{0}$. In this regime, assuming that the underlying local energies linearize properly in the sense that $W^{(r)}(\mathbf{F}, \mathbf{0}) = 1/2(\mathbf{F}-\mathbf{I}) \cdot \mathcal{L}^{(r)}(\mathbf{F}-\mathbf{I}) + O(\|\mathbf{F}-\mathbf{I}\|^3)$ with $\mathcal{L}^{(r)} \doteq \partial^2 W^{(r)}(\mathbf{I}, \mathbf{0})/\partial \mathbf{F} \partial \mathbf{F}$, the effective free energy function (6) of *any* two-phase elastic dielectric composite admits a series expansion of the form

$$\overline{W}(\overline{\mathbf{F}}, \mathbf{0}) = \frac{1}{2}(\overline{\mathbf{F}}-\mathbf{I}) \cdot \tilde{\mathcal{L}}(\overline{\mathbf{F}}-\mathbf{I}) + O(\|\overline{\mathbf{F}}-\mathbf{I}\|^3), \tag{76}$$

where $\tilde{\mathcal{L}}$ is the so-called effective modulus tensor of the composite. When the inhomogeneity $\Delta\mathcal{L} = \mathcal{L}^{(2)} - \mathcal{L}^{(1)}$ between the local moduli $\mathcal{L}^{(r)}$ is small, the tensor $\tilde{\mathcal{L}}$ is given asymptotically (see, e.g., Section III.A in Willis, 1981) by

$$\tilde{\mathcal{L}} = c_0^{(1)}\mathcal{L}^{(1)} + c_0^{(2)}\mathcal{L}^{(2)} - c_0^{(1)}c_0^{(2)}\Delta\mathcal{L}\mathcal{P}^{(1)}\Delta\mathcal{L} + O(\Delta\mathcal{L}^3). \tag{77}$$

Here, it is recalled that $c_0^{(1)}$ and $c_0^{(2)}$ denote the volume fractions of materials $r=1$ and $r=2$, respectively, and $\mathcal{P}^{(1)}$ is a microstructural fourth-order tensor that contains information about the two-point correlation function $p_0^{(22)}$. For *periodic* microstructures (see, e.g., Chapter 14 in Milton, 2002),

$$\mathcal{P}^{(1)} = \sum_{\substack{\mathbf{k} \in \mathcal{R}^* - \{\mathbf{0}\} \\ \boldsymbol{\xi} = \mathbf{k}/|\mathbf{k}|}} \frac{\widehat{p}_0^{(22)}(\mathbf{k})}{c_0^{(1)}c_0^{(2)}} \mathbf{H}^{(1)}(\boldsymbol{\xi}) \quad \text{with } \widehat{p}_0^{(22)}(\mathbf{k}) = \frac{1}{|Q_0|}\int_{Q_0} p_0^{(22)}(\mathbf{X}) e^{-\mathrm{i}\mathbf{X}\cdot\mathbf{k}}\, \mathrm{d}\mathbf{X}, \tag{78}$$

where it is recalled that Q_0 and $\mathcal{R}^*$ stand for the unit cell and reciprocal lattice defining the periodicity of the microstructure. For *random* microstructures (Willis, 1981),

$$\mathcal{P}^{(1)} = -\frac{1}{8\pi^2}\int_{|\boldsymbol{\xi}|=1}\left[\int_{\Omega_0} \frac{p^{(22)}(\mathbf{X}) - (c_0^{(2)})^2}{c_0^{(1)}c_0^{(2)}}\, \delta''(\boldsymbol{\xi}\cdot\mathbf{X})\, \mathrm{d}\mathbf{X}\right] \mathbf{H}^{(1)}(\boldsymbol{\xi})\, \mathrm{d}\boldsymbol{\xi}, \tag{79}$$

where δ'' denotes the second derivative of the Dirac delta function. In the above two expressions,

$$H_{ijkl}^{(1)}(\boldsymbol{\xi}) = N_{ik}^{(1)}(\boldsymbol{\xi})\xi_j\xi_l \quad \text{with} \quad \mathbf{N}^{(1)}(\boldsymbol{\xi}) = [\mathbf{K}^{(1)}(\boldsymbol{\xi})]^{-1}, \quad K_{ik}^{(1)}(\boldsymbol{\xi}) = \mathcal{L}_{ijkl}^{(1)}\xi_j\xi_l, \tag{80}$$

where $\mathbf{K}^{(1)}$ is the so-called acoustic tensor associated with material $r=1$.

Now, given that the result (35)–(36) for $\overline{W}$ is exact for a *specific* class of particulate microstructures, it should reduce to the *general* exact result (81) in the linearly elastic regime. To see this connection, we begin by noting that the effective free energy function defined by (35)–(36) admits as well a series expansion of the form

$$\overline{W}\left(\overline{\mathbf{F}}, \mathbf{0}, c_0^{(2)}\right) = \frac{1}{2}(\overline{\mathbf{F}}-\mathbf{I}) \cdot \overline{\mathbf{L}}\,(\overline{\mathbf{F}}-\mathbf{I}) + O(\|\overline{\mathbf{F}}-\mathbf{I}\|^3) \quad \text{with } \overline{\mathbf{L}} \doteq \frac{\partial^2 \overline{W}}{\partial \overline{\mathbf{F}} \partial \overline{\mathbf{F}}}\left(\mathbf{I}, \mathbf{0}, c_0^{(2)}\right). \tag{81}$$

Setting $\overline{\mathbf{E}}=\mathbf{0}$, making explicit use of the ansatz (81), and expanding about $\overline{\mathbf{F}}=\mathbf{I}$, the initial-value problem (35)–(36) can be shown to reduce to the Riccati ordinary differential equation (ode)

$$\subset \frac{\mathrm{d}\overline{\mathbf{L}}}{\mathrm{d}\subset}-\Delta\overline{\mathbf{L}}-\Delta\overline{\mathbf{L}}\mathbf{P}^{(1)}\Delta\overline{\mathbf{L}}=\mathbf{0}\quad\text{subject to the intial condition}\quad\overline{\mathbf{L}}(1)=\mathcal{L}^{(2)} \tag{82}$$

for the modulus tensor $\overline{\mathbf{L}}$. Here, we have made use of the notation $\Delta\overline{\mathbf{L}}=\overline{\mathbf{L}}-\mathcal{L}^{(1)}$ and

$$\mathbf{P}^{(1)}=\int_{|\boldsymbol{\xi}|=1}\mathbf{H}^{(1)}(\boldsymbol{\xi})\nu(\boldsymbol{\xi})\,\mathrm{d}\boldsymbol{\xi}. \tag{83}$$

Although nonlinear, the Riccati ode (82) can be solved explicitly to render

$$\overline{\mathbf{L}}=\mathcal{L}^{(1)}+c_0^{(2)}[c_0^{(1)}\mathbf{P}^{(1)}+(\Delta\mathcal{L})^{-1}]^{-1}. \tag{84}$$

In the limit of small inhomogeneity as $\Delta\mathcal{L}\to\mathbf{0}$, this result reduces finally to

$$\overline{\mathbf{L}}=c_0^{(1)}\mathcal{L}^{(1)}+c_0^{(2)}\mathcal{L}^{(2)}-c_0^{(1)}c_0^{(2)}\Delta\mathcal{L}\mathbf{P}^{(1)}\Delta\mathcal{L}+O(\Delta\mathcal{L}^3), \tag{85}$$

which is seen to be identical in form to (77) but with the tensor $\mathcal{P}^{(1)}$ replaced by $\mathbf{P}^{(1)}$. Since, again, the result (85) is exact for a specific class of particulate microstructures, it follows by confronting (83) with $(78)_1$ and (79) that the microstructural function $\nu(\boldsymbol{\xi})$ in the result (35)–(36) for $\overline{W}$ is indeed directly related to the two-point correlation function $p_0^{(22)}$ via expression $(38)_1$ for periodic microstructures, and via expression $(42)_1$ for random ones.

Appendix B. Local fields

In addition to the effective free energy function $\overline{W}$, a full characterization of the behavior of elastic dielectric particulate composites requires information on the local fields within the matrix and the particles. For instance, information on the average stress and electric fields within the matrix could be used to infer the onset of local material instabilities such as cavitation and electric breakdown. As sketched out below, such local information can be accessed from the result (35)–(36) with help of a simple perturbation technique (see, e.g., Idiart and Ponte Castañeda, 2006).

Instead of the original problem (10) with local free energy function (2), consider the "perturbed" problem

$$\overline{W}_\tau(\overline{\mathbf{F}},\overline{\mathbf{E}})=\min_{\mathbf{F}\in\mathcal{K}^\sharp}\max_{\mathbf{E}\in\mathcal{E}^\sharp}\int_{\Omega_0}W_\tau(\mathbf{X},\mathbf{F},\mathbf{E})\,\mathrm{d}\mathbf{X} \tag{86}$$

with

$$\begin{aligned}W_\tau(\mathbf{X},\mathbf{F},\mathbf{E})&=[1-\theta_0^{(2)}(\mathbf{X})]W_\tau^{(1)}(\mathbf{F},\mathbf{E})+\theta_0^{(2)}(\mathbf{X})W_\tau^{(2)}(\mathbf{F},\mathbf{E})\\&=[1-\theta_0^{(2)}(\mathbf{X})]\Big[W^{(1)}(\mathbf{F},\mathbf{E})+\tau^{(1)}\mathcal{A}(\mathbf{F},\mathbf{E})\Big]+\theta_0^{(2)}(\mathbf{X})\Big[W^{(2)}(\mathbf{F},\mathbf{E})+\tau^{(2)}\mathcal{A}(\mathbf{F},\mathbf{E})\Big].\end{aligned} \tag{87}$$

Here, $\overline{W}_\tau$ is the effective free energy function of an elastic dielectric composite as defined in Section 2, but with perturbed free energy function (87) describing its local behavior. The function $\mathcal{A}$ is of arbitrary choice and the scalars $\tau^{(1)}$ and $\tau^{(2)}$ are perturbation (material) parameters, such that for $\tau^{(1)}=\tau^{(2)}=0$ the perturbed free energy W_τ reduces to the original free energy W, and thus $\overline{W}_\tau$ reduces to $\overline{W}$. Now, it immediately follows from Hill's lemma that

$$\frac{1}{|\Omega_0^{(r)}|}\int_{\Omega_0^{(r)}}\mathcal{A}(\mathbf{F},\mathbf{E})\,\mathrm{d}\mathbf{X}=\frac{1}{c_0^{(r)}}\frac{\partial\overline{W}_\tau}{\partial\tau^{(r)}}\Big|_{\tau^{(1)}=\tau^{(2)}=0},\quad r=1,2. \tag{88}$$

That is, the volume average of the quantity $\mathcal{A}$ over the matrix ($r=1$) or the particles ($r=2$) in the original elastic dielectric composite with local energy (2) can be determined from the effective free energy function of the composite with perturbed energy (87) via expression (88).

For the class of particulate microstructures considered in Section 3, the function $\overline{W}_\tau=\overline{W}_\tau(\overline{\mathbf{F}},\overline{\mathbf{E}},c_0^{(2)})$ is solution to the pde

$$\subset\frac{\partial\overline{W}_\tau}{\partial\subset}-\overline{W}_\tau-\left\langle\max_{\boldsymbol{\alpha}}\min_{\beta}\left[\boldsymbol{\alpha}\cdot\frac{\partial\overline{W}_\tau}{\partial\overline{\mathbf{F}}}\,\boldsymbol{\xi}+\beta\frac{\partial\overline{W}_\tau}{\partial\overline{\mathbf{E}}}\cdot\boldsymbol{\xi}-W_\tau^{(1)}(\overline{\mathbf{F}}+\boldsymbol{\alpha}\otimes\boldsymbol{\xi},\overline{\mathbf{E}}+\beta\boldsymbol{\xi})\right]\right\rangle=0 \tag{89}$$

with initial condition given by

$$\overline{W}_\tau(\overline{\mathbf{F}},\overline{\mathbf{E}},1)=W_\tau^{(2)}(\overline{\mathbf{F}},\overline{\mathbf{E}}). \tag{90}$$

By differentiating equations (89)–(90) throughout with respect to $\tau^{(r)}$, setting $\tau^{(1)}=\tau^{(2)}=0$ subsequently, and making use of the identity (88), we obtain initial-value problems for the volume average over the matrix or the particles of any desired quantity $\mathcal{A}(\mathbf{F},\mathbf{E})$.

For demonstration purposes, we now employ the above technique to compute the average, $\overline{\mathbf{F}}^{(2)}\triangleq|\Omega_0^{(2)}|^{-1}\int_{\Omega_0^{(2)}}\mathbf{F}(\mathbf{X})\,\mathrm{d}\mathbf{X}$, and second-moment, $\mathcal{M}^{(2)}\triangleq|\Omega_0^{(2)}|^{-1}\int_{\Omega_0^{(2)}}\mathbf{F}(\mathbf{X})\otimes\mathbf{F}(\mathbf{X})\,\mathrm{d}\mathbf{X}$, of the deformation gradient tensor $\mathbf{F}$ within the particles. Making use of the notation $\overline{\mathbf{F}}^{(2)}=\overline{\mathbf{F}}^{(2)}(\overline{\mathbf{F}},\overline{\mathbf{E}},c_0^{(2)})$ and $\mathcal{M}^{(2)}=\mathcal{M}^{(2)}(\overline{\mathbf{F}},\overline{\mathbf{E}},c_0^{(2)})$, the initial-value problem for the average deformation gradient

$\overline{\mathbf{F}}^{(2)}$ is given (in indicial notation) by

$$\subset \frac{\partial \overline{F}_{ij}^{(2)}}{\partial \subset} - \frac{\partial \overline{F}_{ij}^{(2)}}{\partial \overline{F}_{mn}} \langle \alpha_m \xi_n \rangle - \frac{\partial \overline{F}_{ij}^{(2)}}{\partial \overline{E}_n} \langle \beta \xi_n \rangle = 0, \quad F_{ij}^{(2)}(\overline{\mathbf{F}}, \overline{\mathbf{E}}, 1) = \overline{F}_{ij}, \tag{91}$$

and that for the second-moment $\mathcal{M}^{(2)}$ by

$$\subset \frac{\partial \mathcal{M}_{ijkl}^{(2)}}{\partial \subset} - \frac{\partial \mathcal{M}_{ijkl}^{(2)}}{\partial \overline{F}_{mn}} \langle \alpha_m \xi_n \rangle - \frac{\partial \mathcal{M}_{ijkl}^{(2)}}{\partial \overline{E}_n} \langle \beta \xi_n \rangle = 0, \quad \mathcal{M}_{ijkl}^{(2)}(\overline{\mathbf{F}}, \overline{\mathbf{E}}, 1) = \overline{F}_{ij} \overline{F}_{kl}. \tag{92}$$

The vector $\boldsymbol{\alpha}$ and scalar β in these expressions are the maximizing vector $\boldsymbol{\alpha}$ and minimizing scalar β in the original problem (35)–(36) for the effective free energy function $\overline{W}$. Similarly, the average and second-moment of the electric field $\mathbf{E}$ within the particles, written here as $\overline{\mathbf{E}}^{(2)} \doteq |\Omega_0^{(2)}|^{-1} \int_{\Omega_0^{(2)}} \mathbf{E}(\mathbf{X})\, d\mathbf{X}$ and $\mathcal{N}^{(2)} \doteq |\Omega_0^{(2)}|^{-1} \int_{\Omega_0^{(2)}} \mathbf{E}(\mathbf{X}) \otimes \mathbf{E}(\mathbf{X})\, d\mathbf{X}$, can be shown to be given implicitly by the initial-value problems

$$\subset \frac{\partial \overline{E}_i^{(2)}}{\partial \subset} - \frac{\partial \overline{E}_i^{(2)}}{\partial \overline{F}_{mn}} \langle \alpha_m \xi_n \rangle - \frac{\partial \overline{E}_i^{(2)}}{\partial \overline{E}_n} \langle \beta \xi_n \rangle = 0, \quad E_i^{(2)}(\overline{\mathbf{F}}, \overline{\mathbf{E}}, 1) = \overline{E}_i, \tag{93}$$

and

$$\subset \frac{\partial \mathcal{N}_{ij}^{(2)}}{\partial \subset} - \frac{\partial \mathcal{N}_{ij}^{(2)}}{\partial \overline{F}_{mn}} \langle \alpha_m \xi_n \rangle - \frac{\partial \mathcal{N}_{ij}^{(2)}}{\partial \overline{E}_n} \langle \beta \xi_n \rangle = 0, \quad \mathcal{N}_{ij}^{(2)}(\overline{\mathbf{F}}, \overline{\mathbf{E}}, 1) = \overline{E}_i \overline{E}_j. \tag{94}$$

In these expressions, again, $\boldsymbol{\alpha}$ and β are the maximizing vector and minimizing scalar in the original problem (35)–(36). Given the implicit results (91) and (93) for $\overline{\mathbf{F}}^{(2)}$ and $\overline{\mathbf{E}}^{(2)}$, a simple calculation suffices to deduce that

$$\mathcal{M}^{(2)} = \overline{\mathbf{F}}^{(2)} \otimes \overline{\mathbf{F}}^{(2)} \quad \text{and} \quad \mathcal{N}^{(2)} = \overline{\mathbf{E}}^{(2)} \otimes \overline{\mathbf{E}}^{(2)} \tag{95}$$

are solutions of (92) and (94). And hence that the deformation gradient and electric field are uniform and the same within each particle of the elastic dielectric composites defined by the result (35)–(36), as discussed in comment (iii) of Section 3.3 in the main body of the text.

Appendix C. The F and D formulation

Depending on the specific problem at hand, it may be more convenient to utilize the Lagrangian electric displacement $\mathbf{D}$ as the independent electric variable instead of $\mathbf{E}$. This can be done, for instance, by performing partial Legendre transformations (in the pairs $(\mathbf{E}, \mathbf{D})$ and $(\overline{\mathbf{E}}, \overline{\mathbf{D}})$) of the local and effective free energies already defined in Sections 2 and 3 of the main body of the text. Alternatively, one can start out with free energies that depend on $\mathbf{D}$ instead of $\mathbf{E}$ from the beginning and carry out the pertinent calculations for those. In this appendix, we follow the latter approach and summarize the main results.

Microscopic description of the material. Consider the same two-phase particulate composite defined in Section 2, where now the elastic dielectric behaviors of the matrix ($r=1$) and particles ($r=2$) are characterized by "total" Helmholtz free energy functions $\Phi^{(1)}$ and $\Phi^{(2)}$ of the deformation gradient $\mathbf{F}$ and Lagrangian electric displacement $\mathbf{D}$ such that (Dorfmann and Ogden, 2005)

$$\mathbf{S} = \frac{\partial \Phi}{\partial \mathbf{F}}(\mathbf{X}, \mathbf{F}, \mathbf{D}) \quad \text{and} \quad \mathbf{E} = \frac{\partial \Phi}{\partial \mathbf{D}}(\mathbf{X}, \mathbf{F}, \mathbf{D}) \tag{96}$$

with

$$\Phi(\mathbf{X}, \mathbf{F}, \mathbf{D}) = [1 - \theta_0^{(2)}(\mathbf{X})] \Phi^{(1)}(\mathbf{F}, \mathbf{D}) + \theta_0^{(2)}(\mathbf{X}) \Phi^{(2)}(\mathbf{F}, \mathbf{D}). \tag{97}$$

In terms of these quantities, the total Cauchy stress, Eulerian electric field, and polarization (per unit deformed volume) are given by $\mathbf{T} = J^{-1}\mathbf{S}\mathbf{F}^T$, $\mathbf{e} = \mathbf{F}^{-T}\mathbf{E}$, and $\mathbf{p} = J^{-1}\mathbf{F}\mathbf{D} - \varepsilon_0 \mathbf{e}$.

The macroscopic response. Consistent with the choice of $\mathbf{F}$ and $\mathbf{D}$ as the independent variables, it proves convenient to subject the composite — in contrast to (4) — to affine boundary conditions of the form

$$\mathbf{x} = \overline{\mathbf{F}}\, \mathbf{X} \quad \text{and} \quad \mathbf{D} \cdot \mathbf{N} = \overline{\mathbf{D}} \cdot \mathbf{N} \quad \text{on } \partial\Omega_0, \tag{98}$$

where the unit vector $\mathbf{N}$ denotes the outward normal to $\partial\Omega_0$ and the second-order tensor $\overline{\mathbf{F}}$ and vector $\overline{\mathbf{D}}$ are prescribed boundary data. It immediately ensues from the divergence theorem that $\int_{\Omega_0} \mathbf{F}(\mathbf{X})\, d\mathbf{X} = \overline{\mathbf{F}}$ and $\int_{\Omega_0} \mathbf{D}(\mathbf{X})\, d\mathbf{X} = \overline{\mathbf{D}}$, and so the derivation of the macroscopic response of the elastic dielectric composite reduces to finding the average first Piola-Kirchhoff stress $\overline{\mathbf{S}} \doteq \int_{\Omega_0} \mathbf{S}(\mathbf{X})\, d\mathbf{X}$ and average Lagrangian electric field $\overline{\mathbf{E}} \doteq \int_{\Omega_0} \mathbf{E}(\mathbf{X})\, d\mathbf{X}$. The result can be written as

$$\overline{\mathbf{S}} = \frac{\partial \overline{\Phi}}{\partial \overline{\mathbf{F}}}(\overline{\mathbf{F}}, \overline{\mathbf{D}}) \quad \text{and} \quad \overline{\mathbf{E}} = \frac{\partial \overline{\Phi}}{\partial \overline{\mathbf{D}}}(\overline{\mathbf{F}}, \overline{\mathbf{D}}), \tag{99}$$

where

$$\overline{\Phi}(\overline{\mathbf{F}},\overline{\mathbf{D}})=\min_{\mathbf{F}\in\mathcal{K}}\min_{\mathbf{D}\in\mathcal{D}}\int_{\Omega_0}\Phi(\mathbf{X},\mathbf{F},\mathbf{D})\,\mathrm{d}\mathbf{X} \tag{100}$$

is the effective Helmholtz free energy function of the composite. In this last expression, $\mathcal{K}$ stands for a sufficiently large set of admissible deformation gradients, formally given by (7). On the other hand, $\mathcal{D}$ stands for a sufficiently large set of admissible electric displacement fields. We write formally $\mathcal{D}=\{\mathbf{D}:\mathrm{Div}\,\mathbf{D}=0 \text{ in } \Omega_0,\ \mathbf{D}\cdot\mathbf{N}=\overline{\mathbf{D}}\cdot\mathbf{N} \text{ on } \partial\Omega_0\}$. In terms of the macroscopic quantities (99), it follows that $\overline{\mathbf{T}}=\overline{J}^{-1}\overline{\mathbf{S}}\,\overline{\mathbf{F}}^{T}$, $\overline{\mathbf{e}}=\overline{\mathbf{F}}^{-T}\overline{\mathbf{E}}$, and $\overline{\mathbf{p}}=\overline{J}^{-1}\overline{\mathbf{F}}\,\overline{\mathbf{D}}-\varepsilon_0\overline{\mathbf{e}}$, where it is recalled that $\overline{\mathbf{T}}\doteq|\Omega|^{-1}\int_\Omega\mathbf{T}(\mathbf{x})\,\mathrm{d}\mathbf{x}$, $\overline{\mathbf{d}}\doteq|\Omega|^{-1}\int_\Omega\mathbf{d}(\mathbf{x})\,\mathrm{d}\mathbf{x}$, and $\overline{\mathbf{p}}\doteq|\Omega|^{-1}\int_\Omega\mathbf{p}(\mathbf{x})\,\mathrm{d}\mathbf{x}$.

The Euler–Lagrange equations associated with the variational problem (100) correspond to the equations of conservation of linear momentum and Faraday's law:

$$\mathrm{Div}\,\mathbf{S}=\mathbf{0}\quad\text{and}\quad\mathrm{Curl}\,\mathbf{E}=\mathbf{0}\quad\text{in }\Omega_0. \tag{101}$$

The solution to this coupled system of pdes is in general not unique. As discussed within the context of the complementary equations (9), this lack of uniqueness is associated physically with the possible development of electromechanical instabilities. In this regard, we remark that a key advantage of the $(\mathbf{F},\mathbf{D})$–formulation (100) over the $(\mathbf{F},\mathbf{E})$–formulation (6) is that (100) is a *minimization* problem — as opposed to a *minimax* problem — and thus allows to study the development of such instabilities by means of well-established techniques (Geymonat et al., 1993; Bertoldi and Gei, 2011; Rudykh et al., 2013). For instance, the onset of long wavelength instabilities — that is, geometric instabilities with wavelengths that are much larger than the characteristic size of the underlying microstructure — can be readily detected from the loss of strong ellipticity of the effective free energy function (100) as defined by failure of the condition (Spinelli and Lopez-Pamies, submitted for publication)

$$\min_{\|\mathbf{u}\|=\|\mathbf{v}\|=1}[\mathbf{v}\cdot\boldsymbol{\Gamma}(\mathbf{u};\overline{\mathbf{F}},\overline{\mathbf{D}})\mathbf{v}]>0 \tag{102}$$

at some critical deformation gradients $\overline{\mathbf{F}}$ and electric fields $\overline{\mathbf{E}}$ for some pairs of critical unit vectors $\mathbf{u}$ and $\mathbf{v}$. Here, the "generalized" acoustic tensor $\boldsymbol{\Gamma}$ of the elastic dielectric composite is given by

$$\boldsymbol{\Gamma}(\mathbf{u};\overline{\mathbf{F}},\overline{\mathbf{D}})=\mathbf{K}-\frac{2}{(\mathrm{tr}\,\widehat{\mathbf{B}})^2-\mathrm{tr}\,\widehat{\mathbf{B}}^2}\mathbf{R}\left[\left(\mathrm{tr}\,\widehat{\mathbf{B}}\right)\widehat{\mathbf{I}}-\widehat{\mathbf{B}}\right]\mathbf{R}^T, \tag{103}$$

where

$$K_{ik}=\overline{\mathcal{C}}_{ijkl}u_ju_l,\quad R_{ik}=\overline{\mathcal{D}}_{ijk}u_j,\quad \widehat{I}_{ik}=\delta_{ik}-u_iu_k,\quad \widehat{B}_{ik}=(\delta_{ip}-u_iu_p)\overline{\mathcal{B}}_{pq}(\delta_{qk}-u_qu_k) \tag{104}$$

with

$$\begin{aligned}
\overline{\mathcal{C}}_{ijkl}&=\overline{J}^{-1}\overline{F}_{ja}\overline{F}_{lb}\frac{\partial^2\overline{\Phi}}{\partial\overline{F}_{ia}\partial\overline{F}_{kb}}(\overline{\mathbf{F}},\overline{\mathbf{D}}),\\
\overline{\mathcal{D}}_{ijk}&=\overline{F}_{ja}\overline{F}^{-1}_{bk}\frac{\partial^2\overline{\Phi}}{\partial\overline{F}_{ia}\partial\overline{D}_b}(\overline{\mathbf{F}},\overline{\mathbf{D}}),\\
\overline{\mathcal{B}}_{ij}&=\overline{J}\,\overline{F}^{-1}_{ai}\overline{F}^{-1}_{bj}\frac{\partial^2\overline{\Phi}}{\partial\overline{D}_a\partial\overline{D}_b}(\overline{\mathbf{F}},\overline{\mathbf{D}}),
\end{aligned} \tag{105}$$

and the symbol δ_{ij} stands for the Kronecker delta.

Solutions for the effective free energy function $\overline{\Phi}$. In order to generate solutions for (100), we can make use of the very same iterative techniques elaborated in Section 3 of the main body of the text. Omitting details, with help of the notation $\overline{\Phi}=\overline{\Phi}(\overline{\mathbf{F}},\overline{\mathbf{D}},c_0^{(2)})$, the final result can be shown to be given implicitly by the first-order nonlinear pde

$$c\frac{\partial\overline{\Phi}}{\partial c}-\overline{\Phi}-\left\langle\max_{\boldsymbol{\omega}}\max_{\boldsymbol{\gamma}}\left[\boldsymbol{\omega}\cdot\frac{\partial\overline{\Phi}}{\partial\overline{\mathbf{F}}}\boldsymbol{\xi}+(\boldsymbol{\gamma}\wedge\boldsymbol{\xi})\cdot\frac{\partial\overline{\Phi}}{\partial\overline{\mathbf{D}}}-\Phi^{(1)}(\overline{\mathbf{F}}+\boldsymbol{\omega}\otimes\boldsymbol{\xi},\overline{\mathbf{D}}+\boldsymbol{\gamma}\wedge\boldsymbol{\xi})\right]\right\rangle=0 \tag{106}$$

subject to the initial condition

$$\overline{\Phi}(\overline{\mathbf{F}},\overline{\mathbf{D}},1)=\Phi^{(2)}(\overline{\mathbf{F}},\overline{\mathbf{D}}). \tag{107}$$

Here, it is recalled that the triangular brackets denote the orientational average (32) and the integration of the pde (106) is to be carried out from $c=1$ to the desired final value of volume fraction of particles $c=c_0^{(2)}$. Similar to (35)–(36), this result is valid for any choice of free energy functions $\Phi^{(1)}$ and $\Phi^{(2)}$ describing the elastic dielectric behaviors of the matrix and particles. It is also valid for any choice of one- and two-point correlation functions $p_0^{(2)}=c_0^{(2)}$ and $p_0^{(22)}$ describing the microstructure. Again, the dependence on $p_0^{(22)}$ enters through the function $\nu(\boldsymbol{\xi})$, given explicitly by expression $(38)_1$ for periodic microstructures and by $(42)_1$ for random ones.

Application to ideal dielectric composites. For the fundamental case when the matrix and particles are ideal elastic dielectrics with free energy functions

$$\Phi^{(1)}(\mathbf{F},\mathbf{D})=\begin{cases}\dfrac{\mu}{2}(\mathbf{F}\cdot\mathbf{F}-3)+\dfrac{1}{2\varepsilon}\mathbf{F}\mathbf{D}\cdot\mathbf{F}\mathbf{D} & \text{if } J=1\\ +\infty & \text{otherwise}\end{cases} \tag{108}$$

and

$$\Phi^{(2)}(\mathbf{F},\mathbf{D})=\begin{cases}\dfrac{\mu_p}{2}(\mathbf{F}\cdot\mathbf{F}-3)+\dfrac{1}{2\varepsilon_p}\mathbf{F}\mathbf{D}\cdot\mathbf{F}\mathbf{D} & \text{if } J=1\\ +\infty & \text{otherwise}\end{cases}, \tag{109}$$

the solution for the effective free energy function $\overline{\Phi}$ defined by (106)–(107) can be shown to reduce to

$$\overline{\Phi}(\overline{\mathbf{F}},\overline{\mathbf{D}},c_0)=\begin{cases}2\mu\overline{V}\left(\overline{\mathbf{F}},\overline{\mathbf{d}},c_0\right)+\dfrac{\mu}{2}\left[\overline{\mathbf{F}}\cdot\overline{\mathbf{F}}-3\right]+\dfrac{1}{2\varepsilon}\overline{\mathbf{F}}\,\overline{\mathbf{D}}\cdot\overline{\mathbf{F}}\,\overline{\mathbf{D}} & \text{if } \bar{J}=1\\ +\infty & \text{otherwise}\end{cases}, \tag{110}$$

where the notation $c_0=c_0^{(2)}$ has been used for consistency with the $(\overline{\mathbf{F}},\overline{\mathbf{E}})$–version (51) of the same result, $\overline{\mathbf{d}}=\overline{\mathbf{F}}\,\overline{\mathbf{D}}$ denotes the macroscopic electric displacement in the deformed configuration, and the function $\overline{V}$ is solution to the initial-value problem

$$c\frac{\partial\overline{V}}{\partial c}-\overline{V}-\left\langle\frac{\partial\overline{V}}{\partial\overline{\mathbf{F}}}\boldsymbol{\xi}\cdot\frac{\partial\overline{V}}{\partial\overline{\mathbf{F}}}\boldsymbol{\xi}-\frac{\left(\dfrac{\partial\overline{V}}{\partial\overline{\mathbf{F}}}\boldsymbol{\xi}\cdot\overline{\mathbf{F}}^{-T}\boldsymbol{\xi}\right)^2}{\overline{\mathbf{F}}^{-T}\boldsymbol{\xi}\cdot\overline{\mathbf{F}}^{-T}\boldsymbol{\xi}}+\mu\varepsilon\frac{\partial\overline{V}}{\partial\overline{\mathbf{d}}}\cdot\frac{\partial\overline{V}}{\partial\overline{\mathbf{d}}}-\mu\varepsilon\frac{\left(\dfrac{\partial\overline{V}}{\partial\overline{\mathbf{d}}}\cdot\overline{\mathbf{F}}^{-T}\boldsymbol{\xi}\right)^2}{\overline{\mathbf{F}}^{-T}\boldsymbol{\xi}\cdot\overline{\mathbf{F}}^{-T}\boldsymbol{\xi}}\right\rangle=0 \tag{111}$$

with

$$\overline{V}\left(\overline{\mathbf{F}},\overline{\mathbf{d}},1\right)=\frac{1}{4}\left(\frac{\mu_p}{\mu}-1\right)\left[\overline{\mathbf{F}}\cdot\overline{\mathbf{F}}-3\right]+\frac{1}{4\mu}\left(\frac{1}{\varepsilon_p}-\frac{1}{\varepsilon}\right)\overline{\mathbf{d}}\cdot\overline{\mathbf{d}}. \tag{112}$$

Akin to its $(\overline{\mathbf{F}},\overline{\mathbf{E}})$–counterpart (52), the pde (111) exhibits quadratic nonlinearity.

References

Akdogan, E.K., Allahverdi, M., Safari, A., 2005. Piezoelectric composites for sensor and actuator applications. IEEE Trans. Ultrason. Ferroelectrics Freq. Control 52, 746–775.

Avellaneda, M., 1987. Iterated homogenization, differential effective medium theory and applications. Commun. Pure Appl. Math. 40, 527–554.

Avellaneda, M., Milton, G.W., 1989. Bounds on the effective elasticity tensor of composites based on two-point correlations. In: Proceedings of the 12th Energy-Sources Technology Conference and Exhibition: Composite Material Technology, pp. 89–93.

Ball, J.M., 1982. Discontinuous equilibrium solutions and cavitation in nonlinear elasticity. Philos. Trans. R. Soc. A 306, 557–611.

Bar-Cohen, Y. (Ed.), 2001. Electroactive Polymer (EAP) Actuators as Artificial Muscles. SPIE Press.

Bertoldi, K., Gei, M., 2011. Instabilities in multilayered soft dielectrics. J. Mech. Phys. Solids 59, 18–42.

Born, M., Wolf, E., Bhatia, A.B., 2003. Principles of Optics: Electromagnetic Theory of Propagation, Interference, and Diffraction of Light. Cambridge University Press.

Braides, A., Lukkassen, D., 2000. Reiterated homogenization of integral functionals. Math. Models Methods Appl. Sci. 10, 47–71.

Brown, W.F., 1955. Solid mixture permittivities. J. Chem. Phys. 23, 1514–1517.

Bruggeman, D.A.G., 1935. Berechnung verschiedener physikalischer Konstanten von heterogenen Substanzen. I. Dielektrizitätskonstanten und Leitfähigkeiten der Mischkörper aus isotropen Substanzen. (Calculation of various physical constants in heterogeneous substances. I. Dielectric constants and conductivity of composites from isotropic substances). Ann. Phys. 416, 636–664.

Cady, W.G., 1946. Piezoelectricity. McGraw-Hill.

Carpi, F., Smela, E. (Eds.), 2009. Biomedical Applications of Electroactive Polymer Actuators. Wiley.

Danas, K., Kankanala, S.V., Triantafyllidis, N., 2012. Experiments and modeling of iron-particle-filled magnetorheological elastomers. J. Mech. Phys. Solids 60, 120–138.

deBotton, G., 2005. Transversely isotropic sequentially laminated composites in finite elasticity. J. Mech. Phys. Solids 53, 1334–1361.

deBotton, G., Tevet-Deree, L., Socolsky, E.A., 2007. Electroactive heterogeneous polymers: analysis and applications to laminated composites. Mech. Adv. Mater. Struct. 14, 13–22.

Dorfmann, A., Ogden, R.W., 2005. Nonlinear electroelasticity. Acta Mech. 174, 167–183.

Fleming, W.H., Rishel, R., 1975. Deterministic and Stochastic Optimal Control. Springer-Verlag, New York.

Fosdick, R., Tang, H., 2007. Electrodynamics and thermomechanics of material bodies. J. Elasticity 88, 255–297.

Francfort, G.A., Murat, F., 1986. Homogenization and optimal bounds in linear elasticity. Arch. Ration. Mech. Anal. 94, 307–334.

Geymonat, G., Müller, S., Triantafyllidis, N., 1993. Homogenization of nonlinearly elastic materials, microscopic bifurcation and macroscopic loss of rank-one convexity. Arch. Ration. Mech. Anal. 122, 231–290.

Hashin, Z., 1985. Large isotropic elastic deformation of composites and porous media. Int. J. Solids Struct. 21, 711–720.

Hill, R., 1972. On constitutive macrovariables for heterogeneous solids at finite strain. Proc. R. Soc. London A 326, 131–147.

Huang, C., Zhang, Q.M., Li, J.Y., Rabeony, M., 2005. Colossal dielectric and electromechanical responses in self-assembled polymeric nanocomposites. Appl. Phys. Lett. 87, 182901.

Idiart, M.I., 2008. Modeling the macroscopic behavior of two-phase nonlinear composites by infinite-rank laminates. J. Mech. Phys. Solids 56, 2599–2617.

Idiart, M.I., Ponte Castañeda, P., 2006. Field statistics in nonlinear composites. I. Theory. Proc. R. Soc. London A 463, 183–202.

Kofod, G., Sommer-Larsen, P., Kornbluh, R., Pelrine, R., 2003. Actuation response of polyacrylate dielectric elastomers. J. Intell. Mater. Syst. Struct. 14, 787–793.

Leblanc, J.L., 2010. Filled Polymers: Science and Industrial Applications. CRC Press.

Lewis, T.J., 2004. Interfaces are the dominant feature of dielectrics at the nanometric level. IEEE Trans. Dielectr. Electr. Insul. 11, 739–753.

Li, W., Landis, C.M., 2012. Deformation and instabilities in dielectric elastomer composites. Smart Mater. Struct. 21, 094006.
Lopez-Pamies, O., 2010. An exact result for the macroscopic response of particle-reinforced Neo-Hookean solids. J. Appl. Mech. 77, 021016.
Lopez-Pamies, O., Ponte Castañeda, P., 2009. Microstructure evolution in hyperelastic laminates and implications for overall behavior and macroscopic stability. Mech. Mater. 41, 364–374.
Lopez-Pamies, O., Idiart, M.I., Nakamura, T., 2011a. Cavitation in elastomeric solids: I – A defect-growth theory. J. Mech. Phys. Solids 59, 1464–1487.
Lopez-Pamies, O., Nakamura, T., Idiart, M.I., 2011b. Cavitation in elastomeric solids: II — Onset-of-cavitation surfaces for Neo-Hookean materials. J. Mech. Phys. Solids 59, 1488–1505.
Lopez-Pamies, O., Goudarzi, T., Nakamura, T., 2013. The nonlinear elastic response of suspensions of rigid inclusions in rubber: I — An exact result for dilute suspensions. J. Mech. Phys. Solids 61, 1–18.
Maslov, V.P., Fedoriuk, M.V., 1981. Semi-classical Approximation in Quantum Mechanics. Reidel, Dordrecht.
McMeeking, R.M., Landis, C.M., 2005. Electrostatic forces and stored energy for deformable dielectric materials. J. Appl. Mech. 72, 581–590.
Michel, J.C., Lopez-Pamies, O., Ponte Castañeda, P., Triantafyllidis, N., 2010. Microscopic and macroscopic instabilities in finitely strained fiber-reinforced elastomers. J. Mech. Phys. Solids 58, 1776–1803.
Milton, G.W., Kohn, R.V., 1988. Variational bounds of the effective moduli of anisotropic composites. J. Mech. Phys. Solids 36, 597–629.
Milton, G.W., 2002. The Theory of Composites. Cambridge Monographs on Applied and Computational Mathematics, vol. 6. Cambridge University Press, Cambridge.
Norris, A.N., 1985. A differential scheme for the effective moduli of composites. Mech. Mater. 4, 1–16.
Ogden, R.W., 1978. Extremum principles in non-linear elasticity and their application to composites — I Theory. Int. J. Solids Struct. 14, 265–282.
Pelrine, R., Kornbluh, R., Joseph, J.P., 1998. Electrostriction of polymer dielectrics with compliant electrodes as a means of actuation. Sensors Actuators A 64, 77–85.
Pelrine, R., Kornbluh, R., Pei, Q., Joseph, J., 2000. High-speed electrically actuated elastomers with strain greater than 100%. Science 287, 836–839.
Ponte Castañeda, P., Siboni, M.H., 2012. A finite-strain constitutive theory for electro-active polymer composites via homogenization. Int. J. Non-Linear Mech. 47, 293–306.
Razzaghi Kashani, M., Javadi, S., Gharavi, N., 2010. Dielectric properties of silicone rubber-titanium dioxide composites prepared by dielectrophoretic assembly of filler particles. Smart Mater. Struct. 19, 035019.
Roy, M., Nelson, J.K., MacCrone, R.K., Schadler, L.S., Reed, C.W., Keefe, R., Zenger, W., 2005. Polymer nanocomposite dielectrics — the role of the interface. IEEE Transactions on Dielectrics and Electrical Insulation 12, 629–643.
Rudykh, S., Lewinstein, A., Uner, G., deBotton, G., 2013. Analysis of microstructural induced enhancement of electromechanical coupling in soft dielectrics. Appl. Phys. Lett. 102, 151905.
Sethian, J.A., 1999. Level Set Methods and Fast Marching Methods: Evolving Interfaces in Computational Geometry, Fluid Mechanics, Computer Vision, and Materials Science. Cambridge University Press.
Spinelli, S.A., Lopez-Pamies, O. A general closed-form solution for the overall response of piezoelectric composites with periodic and random particulate microstructures, submitted for publication.
Spinelli, S.A., Lopez-Pamies, O. Some simple explicit results for the elastic dielectric properties and stability of layered composites, submitted for publication.
Stratton, J.S., 1941. Electromagnetic Theory. McGraw-Hill.
Suo, Z., Zhao, X., Greene, W.H., 2008. A nonlinear field theory of deformable dielectrics. J. Mech. Phys. Solids 56, 467–486.
Tartar, L., 1985. Estimations fines des coefficients homogénéisés. In: Krée, P. (Ed.), Ennio de Giorgi Colloquium, Research Notes in Mathematics, vol. 125. . Pitman Publishing Ltd., London, pp. 168–187. (Fine estimations of homogenized coefficients.).
Tartar, L., 1990. H-measures, a new approach for studying homogenization, oscillation and concentration effects in partial differential equations. Proc. R. Soc. Edinburgh Sect. London A 115, 193–230.
Tian, L., Tevet-Deree, L., deBotton, G., Bhattacharya, K., 2012. Dielectric elastomer composites. J. Mech. Phys. Solids 60, 181–198.
Toupin, R.A., 1956. The elastic dielectric. J. Ration. Mech. Anal. 5, 849–915.
Uchino, K., 1997. Piezoelectric Actuators and Ultrasonic Motors. Kluwer Academic Publishers.
Vu, D.K., Steinmann, P., 2007. Nonlinear electro- and magneto-elastostatics: material and spatial settings. Int. J. Solids Struct. 44, 7891–7905.
Willis, J.R., 1981. Variational and related methods for the overall properties of composites. Adv. Appl. Mech. 21, 1–78.
Wissler, M., Mazza, E., 2007. Electromechanical coupling in dielectric elastomer actuators. Sensors Actuators A 138, 384–393.
Xiao, Y., Bhattacharya, K., 2008. A continuum theory of deformable, semiconducting ferroelectrics. Arch. Ration. Mech. Anal. 189, 59–95.
Zhang, Q.M., Li, H., Poh, M., Xia, F., Cheng, Z.Y., Xu, H., Huang, C., 2002. An all organic composite actuator material with a high dielectric constant. Nature 419, 284–287.
Zhang, S., Huang, C., Klein, R.J., Xia, F., Zhang, Q.M., Cheng, Z.Y., 2007. High performance electroactive polymers and nano-composites for artificial muscles. J. Intell. Mater. Syst. Struct. 18, 133–145.